

2017

STRIDE

Southeastern Transportation Research,
Innovation, Development and Education Center

Final Report

Signal Timing Optimization with
Consideration of
Environment and Safety Impacts,
Part B

(Project # 2013-022S)



Authors: Gustavo R. de Andrade, Lily Elefteriadou, Ph.D., and Lei Zhang (University of Florida)

June 2017



U.S. DOT DISCLAIMER

The contents of this report reflect the views of the authors, who are responsible for the facts, and the accuracy of the information presented herein. This document is disseminated under the sponsorship of the U.S. Department of Transportation's University Transportation Centers Program, in the interest of information exchange. The U.S. Government assumes no liability for the contents or use thereof.

ACKNOWLEDGEMENT OF SPONSORSHIP

This work was sponsored by a grant from the Southeastern Transportation Research, Innovation, Development, and Education Center (STRIDE) at the University of Florida. The STRIDE center is funded through the U.S. Department of Transportation's University Transportation Centers Program.

CONTENTS

LIST OF FIGURES	6
LIST OF TABLES	7
ABSTRACT	9
CHAPTER 1: BACKGROUND	11
INTRODUCTION	11
OBJECTIVES AND SCOPE	11
STRUCTURE OF THIS DOCUMENT	12
CHAPTER 2: LITERATURE REVIEW	13
PART 1: CRASH PREDICTION MODEL	13
Evolution of Crash Studies at Intersections	13
Simulation Based Methods	19
The Highway Safety Manual	21
The New Zealand Model	26
Summary and Conclusions	28
PART 2: IMPLEMENTATION OF CRASH PREDICTION AND MOBILITY Models INTO MULTIOBJECTIVE FUNCTIONS	34
Genetic Algorithms Basic Concepts	35
Signal Control Optimization	37
Summary and Conclusion	40

PART 3: SENSITIVITY ANALYSIS	41
CHAPTER 3: METHODOLOGY	44
New or Modified Inputs.....	45
Optimization Procedures.....	51
Objective Function.....	52
Operations	54
Safety	56
Emissions	64
Main outputs	64
CHAPTER 4: RESULTS	66
BASE SCENARIO	66
Design	66
Demand.....	67
Safety-only characteristics	68
Control	68
Optimization guidelines	69
SENSITIVITY ANALYSIS	70
Variables	71
Summary of Tested Variables and Ranges	74
Method	75

Data Analysis 78

CHAPTER 5: CONCLUSIONS AND RECOMMENDATIONS 93

REFERENCES 95

LIST OF FIGURES

Figure 1: Scheme of Genetic Algorithm.....	36
Figure 2: Methodology	44
Figure 3: HCS Primary Input Data Screen.....	47
Figure 4: HCS Detailed Input Data / Full Optimization Screen for the Arterial	48
Figure 5. Types and Location of Signal Display	50
Figure 6: Safety and Emissions Screen.....	51
Figure 7. Signalized intersection movement codes (Reference: northbound direction)...	57
Figure 8. Spreadsheet built to validate HCS implementation – Inputs and calculations..	63
Figure 9. Spreadsheet built to validate HCS implementation – Outputs	63
Figure 10. New Output Screen.....	65
Figure 11: Configuration and Demand on Testing Arterial	67
Figure 12: Configuration and Demand on Testing Arterial	70
Figure 13: Variability of μ for each variable – Delay	80
Figure 14: Variability of μ for each variable – Crashes	85
Figure 15: Variability of μ for each variable – Emissions	90

LIST OF TABLES

Table 1. Crash Type Definition	14
Table 2. Crash Reduction Factors	23
Table 3. Distribution of Multiple-Vehicle Collisions for Intersections by Collision Type	25
Table 4. Types of Relationships Based on the Model’s Coefficients	27
Table 5. Selected Model Details	31
Table 6. Right-angle crash (all day).....	58
Table 7. Left-turn-against crash (all day)	59
Table 8. Rear-end crashes (all day, for all sizes of intersections).....	60
Table 9. Loss-of-control crashes.....	61
Table 10. Other crashes.....	62
Table 11. Initial Signal Timing Plan.....	69
Table 12. Variables Included in the Sensitivity Analysis and Variation Range.....	75
Table 13. Random Trajectory Generator	76
Table 14. Ranking of μ for the All Variables and Associated β – Delay	79
Table 15. Ranking and Confidence Interval of μ^* for All Variables – Delay	81
Table 16. Kruskal Wallis Test – Delay.....	83
Table 17. Ranking of μ for the All Variables and Associated β – Safety.....	84
Table 18. Ranking and Confidence Interval of μ^* for All Variables – Safety	86
Table 19. Kruskal Wallis Test – Safety	87
Table 20. Ranking of μ for the All Variables and Associated β – Emissions	88

Table 21. Ranking and Confidence Interval of μ^* for All Variables – Emissions 91

Table 22. Kruskal Wallis Test – Emissions 92

ABSTRACT

The main performance measures used in the assessment and optimization of traffic signal timing have traditionally been restricted to mobility, with limited consideration of environmental and safety aspects. The goal of this study is to develop a signal timing optimization algorithm that can consider mobility, safety, and environmental measures simultaneously on coordinated arterials. The objectives of the research are to a) review relevant research that can be used to evaluate safety at signalized intersections as a function of various signalization-related parameters; b) select or develop a set of equations that can be used to predict crashes as a function of intersection characteristics and signal control; c) develop a methodology for optimizing signal control in terms of safety (crashes), environmental impacts (emissions) and operations (delay); d) implement the proposed methodology in the Highway Capacity Software; and e) conduct a sensitivity analysis of the model results to assess the optimal performance measures obtained as a function of key variables that affect mobility, safety and emissions outputs.

Optimization results and statistical analysis of the sensitivity scenarios showed that the effect of each variable on the overall performance of the model is highly dependent on other variables. For instance, the use of shared turns and permitted left could improve both mobility and safety to a degree which is a function of the traffic volumes and turning percentage levels. The size of the intersection, defined as a function of the number of lanes on the arterial, was found to be the most significant variable in the model, largely affecting all performance measures.

The methods developed in this study have been implemented in the Highway Capacity Software (HCS), and can be used to optimize signal control by simultaneously considering mobility, safety, and environmental effects.

CHAPTER 1: BACKGROUND

INTRODUCTION

Transportation agencies are increasingly realizing the importance of performance measurement and management. However, the main performance measures used in the assessment and optimization of signal timing have been mobility measures only (such as delay, stops etc.), with limited consideration of safety and environmental impacts. Consideration of these measures is important, particularly with the increased emphasis on accounting for multiple performance measures in the management of transportation systems.

OBJECTIVES AND SCOPE

The goal of this project is to develop an algorithm capable of generating appropriate signal timing plans to simultaneously improve mobility (average overall delay on intersections and coordinated arterials), emissions (total g of gases) and safety (crash frequency). This report focuses on the mobility and safety components of this goal. The objectives of the research are to:

- a) review relevant research that can be used to evaluate safety at signalized intersections as a function of various signalization-related parameters;
- b) select or develop a set of equations that can be used to predict crashes as a function of intersection characteristics and signal control;
- c) develop a methodology for optimizing signal control in terms of safety (crashes), environmental impacts (emissions) and operations (delay);

- d) implement the proposed methodology in the Highway Capacity Software; and
- e) conduct a sensitivity analysis of the model results to assess the optimal performance measures obtained as a function of key variables that affect mobility, safety and emissions outputs.

STRUCTURE OF THIS DOCUMENT

The next chapter of the report (Chapter 2) summarizes the literature review, focused on crash prediction models for intersections, the genetic algorithm that was applied to solve the proposed problem, and the sensitivity analysis method selected for this work. Chapter 3 describes the methodology framework and its implementation in the Highway Capacity Software (HCS). Chapter 4 presents the results, including the base scenario and the sensitivity analysis. Chapter 5 summarizes the conclusions of the research, limitations of this study and recommendations for future work.

CHAPTER 2: LITERATURE REVIEW

The first part of this chapter summarizes the existing work on crash prediction functions, culminating with the selection of the model for the project purpose. The second part reviews the literature on genetic algorithms that can be used to achieve the goal of this research. The third part discusses the sensitivity analysis methodology selected to analyze the results of this work.

PART 1: CRASH PREDICTION MODEL

This subsection describes the evolution of crash prediction models at intersections over the years and techniques used to build these models, from basic statistical analysis to simulation, the Highway Safety Manual (HSM), and a more recent model that considers signal operations at a higher level of detail. The final subsection summarizes the findings of this review.

Evolution of Crash Studies at Intersections

Crashes at intersections are generally categorized into rear end, sideswipe (same direction), sideswipe (opposite direction), right-angle, head-on/angular, and left-turn/approach-turn crashes. Definitions are shown in Table 1.

Table 1. Crash Type Definition

Type	Definition
Rear-end	Two vehicles, travelling in the same direction and aligned to one another, collide regardless of what movement either vehicle is making, except when one or both vehicles are backing.
Sideswipe	Two vehicles, moving alongside each other, collide laterally. This type would include a collision resulting from one of the vehicles making an improper turn, lane change, or overtaking maneuver, in the same or opposite direction.
Right-angle	A crash where two vehicles, approaching from non-opposing angular directions, collide and impact at an angle. Typically crashes result from vehicles failing to either stop or yield the right of way from a stop or yield sign, running a red light, or not being able to pass through intersections when the green signal of conflicting movements is on.
Head-on	Two vehicles, approaching opposite directions that intend to continue in opposite directions, collide in a frontal or angular manner. This includes collisions resulting from vehicles traveling the wrong way down divided highways or because of loss-of-control.
Loss-of-control	A single vehicle exit the roadway because of loss-of-control over the vehicle. If no escape areas exist, which is the case in most urban settings, the vehicle generally hits a fixed object on the roadside, a parked vehicle, pedestrian, or bicycle.
Approach-turn/ Left-turn	Vehicles traveling in opposite directions on the same street with one vehicle attempting to turn left or U turn in front of the opposing vehicle.

Source: (1) State of New Jersey Department of Transportation.
(2) Minimum uniform crash criteria.
(3) City of Fort Collins.

Poch & Mannering's (4) study is one of the earliest that examined the impact of signal control parameters on intersection safety. A negative binominal (NB) regression model was used. The dataset included 63 intersections over six years and was used to develop four statistical models for different crash categories: (a) all accidents; (b) rear-end accidents; (c) angle accidents; (d) approach-turn accidents. Model coefficients for significant variables were calculated, as well as elasticities to explanatory variables. Results show that two-phase signals increase the frequency of rear-end and angle accidents, but are still safer than unsignalized

intersections in terms of total accidents; and eight-phase signals increase rear-end and approach-turn accidents, for a higher total number of crashes as compared to unsignalized intersections. However, the model only considered two-phase and eight-phase controls. The authors indicate that eight-phase signals are often used under high volumes and heavy congestion traffic conditions. Therefore, increased crashes may be caused by high volumes rather than the number of phases. There is no discussion in this paper about the interaction of those two factors.

In addition, protected left turns could help relieve crash frequency. A protected / permissive left turn is beneficial for reducing rear-end and angle accident accidents, however the total number of crashes could increase. The advantages of this research are: a) crashes are analyzed by types rather than just in total or by vehicle types; b) the authors discuss the limitation of applying Poisson regression model to the over-dispersed crash data. One of the assumptions of Poisson regression is that the mean and variance of data are the same. However, generally, the crash data at different intersections or during different years violates this assumption. Improper application would lead to underestimation of coefficients.

The limitations of this research are: a) it only considered isolated intersections and did not include any variables related to signal coordination and arterial operations; b) there are some variables that were not considered in their entire feasible ranges. For example, it only considers two phase and eight phase control.

In 2007, Mitra et al. (5) studied right angle and rear-end crashes in Singapore from 1992 to 1999 using a zero-inflated probability model. This model can deal with an instance where data contains many zero counts (cases at a given location and during a period when there is no record of an accident). The method assumes that there are two states: one is called “perfect state”, which assumes the only possible observation is zero, with a probability p ; and other is called “imperfect

state”, which assumes that a Poisson/NB random variable is observed with a probability of $1-p$ (6). Sometimes p and λ (mean of imperfect state) are uncorrelated, but other times p is a simple function of λ as in $p = \frac{1}{1+\lambda^\tau}$ for an unknown constant τ . The former is called zero-inflated Poisson (ZIP) or zero-inflated negative binomial (ZINB) and the latter ZIP(τ) or ZINB(τ).

The data includes crashes from 1992 to 1999 at 52 intersections. A total of 32 explanatory variables represent geometric, traffic controls, and regulatory factors at the intersections. For head-to-rear accidents, the Poisson regression’s assumption was found to be better than the NB’s, but for rear-to-side accident, NB was preferred. For both models, τ was considered insignificant.

Results show that adjacent intersections within 200 meters and existence of bus stops along approaches would decrease head-to side accidents. The number of rear-to-rear accidents would increase with higher speed limits and surveillance cameras, and decrease with adaptive signal controls. Additionally, presence of uncontrolled left-turn channels, existence of medians wider than 6.56 ft (2 meters), higher approach volumes, and more phases per cycle would all contribute to higher instances of accidents by both maneuver types.

Chin and Quddus (7) were concerned that crash data could be related in time and space. Therefore, a random effect NB model is more proper than both a Poisson and NB model, since the latter models require accident data to be uncorrelated. Their study included 832 observations over 7 years and showed that the increased number of phases per cycle might have increased the number of accidents. Moreover, adaptive signal controls appeared to have an effect in reducing accident occurrence. Although this study applied an advanced model, it did not consider different crash types.

Wang and Abdel-Aty (8) agree that there are temporal and spatial correlations among crash data. Temporal crash data are observations at a cross section of an intersection over several periods of time. By considering the temporal effect, it is possible to explore the effectiveness of the change of certain explanatory variables. For the spatial dimension, the authors suggested that intersections within a given range might be correlated because of factors such as traffic coordination and platoons. Therefore, intersections were grouped into clusters using a distance criterion. Intersections within a cluster were considered to be spatially correlated, and those from different clusters were assumed to be statistically independent.

The authors point out that using either Poisson or NB models for longitudinal data may be problematic, because both assume that the crash data (e.g. the annual number of crashes at each intersection) are independent, which conflicts with the assumption stated previously. Moreover, errors of crashes within the same intersection should be highly correlated, while errors amongst different intersections are random. In that sense, these two models could not describe the error structure correctly. Generalized estimating equations (GEE) were applied with a NB link function with four correlation structures such as independent, exchangeable, auto-regressive, and unstructured.

The explanatory variables are geometric design features, traffic characteristics, traffic control, and operational features. For temporal analysis, the dependent variable is the number of annual rear-end crashes. For the spatial analysis, the dependent variable is the number of rear-end crashes over two years. The data used for temporal analysis included 208 intersections over 3 years, and the data used for spatial analysis involves 476 intersections along 41 corridors.

The variable that was related with signal timing is left-turn protection on the major/minor roadway. Results showed that the auto-regression structure assumption had the highest R^2 for

both temporal and spatially correlated models. However, this approach could not combine the temporal and spatial correlations into one single model, and the cluster category which is determined by distance in the spatial-correlated model has not been clearly explained and standardized. Also, the correlation categorized by distance may vary from city to city.

A study conducted by Agbelie et al (9) investigated impacts of signal timing parameters, traffic and highway geometric characteristics on crash frequencies at urban signalized intersections. The dataset included 381 urban signalized intersections in Illinois, which were collected from 2004 to 2010. The variables related to signal control included: 1) minimum green time; 2) average green time; 3) maximum green time; 4) types of signal controls (pre-timed or demand-actuated); and 5) the number of phases. It was found that only two factors were statistically significant: the maximum green time and the number of signal phases. Other traffic and geometric variables included in the study were the ratio of major road AADT to that of the minor road and the number of lanes on each approach.

Both Poisson and random-parameters NB models were considered to describe the nature of crash frequencies. The latter model takes into account the possible heterogeneity that may result from one intersection to another and across different data collection periods. Results suggested that the latter model described better the studied phenomenon. The model corroborates results from previous research, as it shows that a unit increase in the number of signal phases would increase crash frequencies by 40%. Additionally, the model indicates that an increase in the maximum green time would increase crash frequencies at signalized intersections with a probability of 93.32%.

Simulation Based Methods

The first studies exploring the potential of microscopic simulation tools to study safety measures in signalized intersections were conducted in the early 2000's (10, 11). As a major conclusion, the authors indicated that there should be a relationship between crash field data and road user interactions, measured in the form of conflicts. Conflicts, in turn, are associated with operational measures such as delays and the number of stops.

Archer (12) investigated more deeply the nature of conflicts from the safety perspective, defining surrogate traffic safety indicators: Time to Accident, Time to Collision, and Post-Encroachment Time. Although those measures were consistent with field data, the simulation model underestimated the corresponding field values. Based on this possibility, subsequent studies emphasize the importance of calibration and validation of traffic microscopic simulation tools for the purpose of generating surrogate safety measures (13, 14), such as the Time-to-Collision, and the Federal Highway Administration (FHWA) now provides a model to relate traffic conflicts to crash rates, the Surrogate Safety Analysis Model – SSAM (15).

More recently, other authors reconsidered whether microsimulation could be used to evaluate intersection safety. Saleem et al. (16) simulated conflicts in four-leg intersections using VISSIM and Paramics. The coefficient estimates for the conflict variables from both models were similar and statistically significant. The second part of the analysis examined the possible effects of left-turn phasing, indicating that the protected–permissive treatment could reduce angle and left turning crashes. However, the new crash–conflict relationships were different from those recommended by the SSAM (15).

Essa and Sayed (17) also found different relationships from those proposed by the SSAM, by calibrating VISSIM to produce conflicts. The calibration process consisted of matching actual field conditions, and the use of sensitivity analysis followed by a genetic algorithm procedure to calibrate the VISSIM parameters that had the biggest effect on the simulated conflicts.

Building new relationships between conflicts and crashes using the microscopic simulator VISSIM was also the objective of a recent study by Shahdah, Saccomanno and Persaud (18), who simulated the effects of countermeasures to left-turn against crashes, using a sample of intersections located in Toronto, Canada. Results obtained from traffic conflicts surrogate safety measures were consistent with those obtained from a rigorous, conventional Empirical Bayes before and after analysis, which is the traditional, albeit costly method of performing such analysis. This study used SAAM relationships and as the surrogate measure the Time-to-Collision (TTC), defined as the time separation between two vehicles before they collide, if both vehicles continue at their present speeds along their respective trajectories. By using this measure, the research tested the impact of protected versus permissive left-turns, and the reduction factor for the number of crashes was estimated as 0.919.

Other factors investigated in the literature included the speed limit. Pirdavani et al. (19) used microsimulation to evaluate the safety of signalized 4-leg intersections and concluded that driver behavior was highly influenced by increasing speed limits, as evidenced by the observed deterioration in surrogate safety metrics.

Stevanovic et al. (20) proposed a method for traffic signal timing based on the optimization of Pareto Fronts. Three dimensions were considered: mobility, environment (emissions) and safety. Safety was accounted for in terms of surrogate measures, using the traffic

microsimulation software VISSIM to calculate potential conflicts in the intersections. A genetic algorithm was implemented to solve the optimization problem, supported by data collected in 5 signalized intersections along a segment in West Valley City, Utah. It was concluded that the process of finding optimum solutions considering mobility, safety and emissions is feasible, and the proposed method could improve signal timings in most cases, as compared to the situation observed in the field. According to the authors, the optimum balance between mobility, safety and emissions did not seem to produce timings which are very different from each other. The variability of safety, for instance, ranged from 5% and 35% in terms of number of conflicts.

The rapid evolution shown in more recent studies regarding simulation-based models suggest that this method might be superior to analytical methods for determining the impact of specific factors to safety. To investigate this, So et al. (21) compared AADT-based crash estimation (approach a) and SAAM simulated conflicts-based (approach b) models. Also, three new approaches were proposed: an integrated approach of simulated conflicts and volume parameters (c); an estimated conflicts-incorporated SPF approach (d); and an intersection operational attribute-based SPF approach (e). Trade-offs between accuracy and practicality of the five models were discussed. It was concluded that approaches (c) and (a) were the best in terms of prediction performance and practicality, respectively. The appropriate choice of model would depend on the availability of resources and objectives of the analyst.

The Highway Safety Manual

Many states have developed crash reduction factors (CRF) for cost-benefit analysis and other purposes, some developed by crash types and severity types as subclasses. The CRFs are

usually estimated using a before-and-after methodology or simulation technique, as discussed previously. As a rule, the CRFs are defined as:

$$CRF = \frac{\text{Crash Rate Before} - \text{Crash Rate After}}{\text{Crash Rate Before}} \times 100 \quad (1)$$

$$\text{Crash Rates} = \frac{\text{Total number of Crashes}}{\text{Exposure}} \quad (2)$$

where *Exposure* is usually calculated in million vehicle-miles (MVM) of travel. Table 2 shows the factors concerning signal controls in Florida as an example.

A positive value of CRF indicates an increase of the total crashes with the implementation of an improvement. If multiple improvements are applied to the same project location, the composite CRF can be estimated as:

$$CRF = CRF_1 + (1 - CRF_1)CRF_2 + (1 - CRF_1)(1 - CRF_2)CRF_3 + \dots \quad (3)$$

Much work has been focused on developing crash prediction models able to make use of adjustment factors in the format of the presented CRF. Among these methodologies, the most comprehensive one is AASHTO's HSM (23). The HSM provides safety performance functions (SPF) to estimate an expected average crash frequency. For intersections, it categorizes crashes into two severity types: fatal-and-injury and property-damage-only crashes. The model considers the types of intersections (by number of legs/approaches) at urban arterials and highways, their geometric design parameters, and traffic control features. The overall formula for predicting the number of accidents is:

Table 2. Crash Reduction Factors

State	Factors	Crash type	Reduction factor (%)
Florida	New signal at channelized intersection	Rear-end	-51
		Angle	53
		Left-turn	34
		Right-turn	70
		Sideswipe	10
		Head-on	53
	New signal at non-channelized intersection	Rear-end	-5
		Angle	11
		Left-turn	34
		Right-turn	23
		Sideswipe	23
		Head-on	-46
	Modify signal timing and phasing	Rear-end	-22
		Angle	31
		Left-turn	66
		Right-turn	-20
		Sideswipe	-17
		Head-on	100

Source: (22) Florida Department of Transportation, <http://www.dot.state.fl.us/rddesign/OA/Tools.shtm>

$$N_{pi} = C_r [(N_{bimv} + N_{bisv})(CMF_{1i} \times \dots \times CMF_{ni}) + N_{pedi}(CMF_{1p} \times \dots \times CMF_{np}) + N_{bikei}] \quad (4)$$

where: C_r = calibration (scaling) factor for a specific roadway segment that is developed for use in a particular geographical area;

N_{bimv} = predicted crash frequency under base conditions involving multiple vehicles.

N_{bimv} = predicted crash frequency under base conditions involving single vehicles.

N_{pedi} & N_{bikei} = predicted average crash frequencies of vehicle-pedestrian collisions and vehicle-bicycle collisions; and

$CMF_1 \dots CMF_n$ = crash modification factors a given type of accident.

The difference between the CMF structure used by the HSM and the CRF presented previously is that while the second represents a percent before-after difference in the total number of accidents, the first is a multiplicative factor applied to the number of accidents predicted for base conditions to account for a series of road or environmental characteristics. Note that, in spite of the name, “crash reduction factors”, they may also represent an increase in the number of crashes, when it has a negative sign. Finally, sometimes the term “accident modification factor” (AMF) is used as a synonym to CMF, to describe multiplicative factors which haven’t been included in the AASHTO’s Highway Safety Manual. This report generally uses the term “CMF”.

Although very comprehensive in nature, the methodology presented by the HSM was conceived for planning and design purpose (23), and does not consider signal control in detail. Factors that are considered in the signalization-related models are oriented towards the geometric and traffic signal control features. For urban intersections, the influencing factors of the model are (HSM, 2010):

- a) Number of intersection legs (3 or 4);
- b) Number of approaches with an intersection left-turn lane (1 to 4 approaches);
- c) Number and type of left-turn signal phasing (permissive; protected/permissive or permissive/protected; or protected);
- d) Number of approaches with intersection right turn lane (all approaches, 0 to 4 approaches);
- e) Number of approaches with right-turn-on-red operation prohibited;

- f) Presence/absence of intersection lighting;
- g) Red-Light Cameras to enforce red signal violations.
- h) Maximum number of traffic lanes to be crossed by a pedestrian in any crossing maneuver at the intersection considering the presence of refuge islands;
- i) Bus Stop within 1,000 ft of the center of the intersection (1 to 3 stops);
- j) Schools within 1,000 ft of the intersection;
- k) Alcohol Sales Establishments within 1,000 ft of the intersection (1 to 9)

Of these, (b), (c), (d) and (e) are related to signal operations and control.

For rural two-lane and multilane highways signalized intersections, the factors related to operations are only the presence of left-turn lanes and right-turn lanes.

Five collision types are defined in the HSM, although the number of predicted accidents refer to the total of crashes. The default proportion of the frequency for each crash type, if needed, is based on site types (Table 3).

Table 3. Distribution of Multiple-Vehicle Collisions for Intersections by Collision Type

Manner of Collision	Proportion of Crashes by Severity Level for Specific Intersection Types							
	3ST		3SG		4ST		4SG	
	FI	PDO	FI	PDO	FI	PDO	FI	PDO
Rear-End	0.421	0.440	0.549	0.546	0.338	0.374	0.450	0.483
Head-on	0.045	0.023	0.038	0.020	0.041	0.030	0.049	0.030
Angle	0.343	0.262	0.280	0.204	0.440	0.335	0.347	0.244
Sideswipe	0.126	0.040	0.076	0.032	0.121	0.044	0.099	0.032
Other	0.065	0.235	0.057	0.198	0.060	0.217	0.055	0.211

Notes: 1. 3ST: Three-leg unsignalized intersection

Source: Highway Safety Manual, 2010 p12-32.

3SG: Three-leg signalized intersection
 4ST: Four-leg unsignalized intersection
 4SG: Four-leg signalized intersection
 FI: Fatal and injury accidents
 PDO: Property damage only

The New Zealand Model

The New Zealand transport agency developed models to predict different types of crashes as a function of traffic operation and geometric factors (24). This study produced comprehensive and systematic crash prediction models by crash type. The categories of crash were: left-angle crashes (right-angle in the U.S.), right-turn-against crashes (left-turn in the U.S.), rear-end crashes, loss-of-control crashes, and other crashes.

The signal control parameters considered were: 1) green time for through movements; 2) yellow time for approaches; 3) all-red for approaches; 4) cycle time for intersections; 5) degree of saturation; 6) total lost time; 7) presence of detectors and coordination with upstream intersections; 8) types of phasing (standard/split/combined); 9) free right-turn on red; 10) phasing types (fully protected/partially protected/filtered).

Prediction models were developed by using generalized linear models, which were widely used in crash modelling. The models follow the format of the HSM models, in which a base location base factor is multiplied by a series of variables that are a function of traffic, operations, and geometry characteristics:

$$A = b_0 x_1^{b_1} x_2^{b_2} \dots x_n^{b_n} \quad (5)$$

where: The dependent variable A is typically the total number of accidents in a 5-year period;

b_0 is the constant adjustment factor of the model, analogous to the HSM C_r factor. In the original document by Turner (24), this parameter was city-specific. It is therefore desirable that b_0 values are calibrated to account for local conditions. However, a default range of values for

this factor is given in the study. For testing purposes, the median of these defaults is used in this work.

x_i are the independent variables. One or more of them is always the annual flow rate for specific movements, while the others are non-flow variables;

b_i are the model coefficients. A log-linear transformation is made as:

$$\log A = \log(b_0 x_1^{b_1} x_2^{b_2} \dots x_n^{b_n}) = \log b_0 + b_1 \log x_1 + b_2 \log x_2 + \dots + b_n \log x_n \quad (6)$$

There are five types of relationships based on the value of coefficients, shown in Table 4.

Table 4. Types of Relationships Based on the Model's Coefficients

Exponent	Relationship with crash rate
$b_i > 1$	Crashes increase as the values of variables increase
$b_i = 1$	Crashes increase at a constant rate as values of variables increase
$0 < b_i < 1$	Crashes increase at a decreasing rate as values of variables increase
$b_i = 0$	The number of accidents are independent of the value of variables
$b_i < 0$	Crashes decrease as the values of variables increase

Data were collected at 238 signalized intersections over 5 years, and crashes were classified according to type. Crash frequencies estimated by these models are the annual mean number of crashes.

This study (24) also considered many factors concerning signal timing, through some of them were found not to be statistically significant and were not included in the final models.

Moreover, the models are straightforward and can be applied easily. The weakness of the models is in the definition of other crashes, which represents a wide variety of crashes that were not completely understood. Also, as with the HSM, the models should be location-specific, as each equation has a constant term, which was calibrated for New Zealand cities; this term should be calibrated locally.

Summary and Conclusions

Although considerable amount of work has been conducted to investigate safety at signalized intersections, those studies usually use statistical distributions to analyze the relationships between geometry and crashes. Since the 1990's, new research started to incorporate operations and control characteristics to the analysis (4). Also, most studies typically focus on specific explanatory variables or safety countermeasures and their impact to a specific type of crash, such as rear-end or left-turn.

Several subsequent studies (5-9) revealed a consensus regarding the relationship between crash rates with some signal parameters such as cycle length, number of phases per cycle, signal control types (pre-timed and adaptive control), coordination, left-turn phasing types (protected/permission), and increased yellow/AR intervals.

An increase in the number of phases per cycle is commonly regarded as harmful for intersection safety. Chin and Quddus's study (7) showed that it would increase the total number of crashes (coefficient is 0.1108), and Agbelie et al. (9) found a similar result (coefficient is 0.076). Poch and Mannering (4) thought that an appropriate and small number of phases such as two-phase signal controls would relieve the total number of crashes (coefficient is -0.055) but

eight-phase would increase crashes (coefficient is 0.285). For rear-end crashes as well as right-angle crashes, both two-phase and eight phase would increase crashes. Mitra et al. (5) also found similar results for rear-end and right-angle crashes. Signal control coordination may improve mobility and reduce the total number of crashes (7).

Studies in the last decades have shown that protected left-turn phasing is helpful in reducing the total number of crashes (4), rear-end (4), right-angle (4), and left-turn crashes (23). Interestingly however, Poch & Mannering (4) found that a protected /permissive left-turn phase would increase the number of left-turn crashes compared with no-signal control. In addition, Wang's study (8) showed that left-turn protection on minor streets may increase rear-end crashes.

Since the early 2000's, more advanced techniques using microscopic traffic simulation tools were used to reconsider the interactions of safety and operation at intersections from another perspective. These studies (10-21) discuss the calibration and validation of microsimulation models to produce surrogate measures to estimate crashes, based on traffic conflicts. Similar to previous research, the intent of many of those studies is to evaluate the impact of specific explanatory variables (countermeasures), not providing the user with means to replicate the model results.

The HSM (23) was the first to present comprehensive multivariate models to evaluate safety on rural and urban intersections by using multiple explanatory variables and regression models to predict crashes. In spite of that, few control parameters are considered. The work conducted by the New Zealand transport agency (24) moved one step ahead by combining operational and geometry parameters to estimate crashes by type.

There are still a few signal parameters that have not been studied, including detector extension time, and the minimum and maximum green times. An extension time should be long enough to ensure a vehicle can enter and clear the intersection safely. Green time duration could be important, especially for intersections with coordinated signal controls, as platoons of vehicles with similar speeds are formed and travel through each intersection. Shorter maximum green times would not only disrupt the platoon formation, but may result in higher numbers of rear-end crashes. Lastly, some types of crashes have not been studied fully such as sideswipe, head-on and run-off crashes.

Regarding existing work on intersection safety related to signal control factors, models developed by Poch & Mannering (4) and Turner (24) are preferable for use in optimization, as they are straightforward and easy to implement as part of a larger model. In a preliminary analysis, Poch's (4) model had advantages as compared to Turner's (24). First, its NB model considers the positive nature of crash frequencies while the generalized linear regression model does not. Also, Turner's study (24) was conducted in New Zealand, and every model includes a constant term, which is location (city) specific. However, Turner's model considers a larger number of operational features, while keeping a simple structure that is more modern and compatible to the HSM CMF structure. This structure has the advantage of allowing for the calibration of existing factors and inclusion of new CMFs, that could be derived from before-after studies using real data or microsimulation, as discussed previously. Therefore, Turner's model was preferred for this work, and Table 5 presents all factors considered by the model and the corresponding CMFs, by crash type. As discussed earlier, CMFs below 1 reduce crashes, while values above 1 increase them.

Table 5. Selected Model Details

Factors	CMF
Right-angle crash (off-peak period)	
Daily volume of through vehicles on approach	factor ^{0.311}
Daily volume of through traffic coming from left side + Daily volume of through traffic coming from right side	factor ^{0.362}
Number of approaching lanes	exp(.356×factor)
Intersection depth	factor ^{0.602}
Cycle time	factor ^{0.037}
All-red	factor ^{-0.636}
Split-phasing	0.69
Mast arm display	0.74
Coordinated	1.31
Advanced detector	2.06
Shared-turns	1.19
Median island	0.67
Right-angle crash (peak period)	
Daily volume of through vehicles on movement 2	factor ^{0.156}
Daily volume of through traffic coming from left side + daily volume of through traffic coming from right side	factor ^{0.381}
Number of approaching lanes	exp(.788×factor)
Intersection depth	factor ^{1.237}
Cycle time	factor ^{-0.945}
All-red	factor ^{-2.528}
Split-phasing	0.35
Mast-arm display	0.56
Coordinated	1.49
Shared-turns	2.06
Median island	1.19
Left-turn crash (off-peak period)	
Daily volume of left-turning vehicles on movement 7	factor ^{0.155}
Left-turn storage length	(1+factor) ^{-0.124}
Number of through lanes	exp (0.352×factor)
Degree of saturation	factor ^{0.397}

Cycle length	factor ^{-0.683}
Full LT Protection	0.71
Shared LT	0.72
Med island	1.22
Cycle facilities	1.35
Left-turn crash (peak period)	
Daily volume of left-turning vehicles on movement 7	factor ^{0.256}
Left-turn storage length	(1+factor) ^{-0.24}
Number of through lanes	exp (0.26×factor)
Degree of saturation	factor ^{0.41}
Cycle length	factor ^{-0.34}
Full LT Protection	0.24
Shared LT	0.56
Med island	1.22
Rear-end crash (off-peak period & small intersection)	
Total AADT entering the intersection from the approach	factor ^{0.447}
Left-turn storage length	(1+factor) ^{-0.259}
Lost time	factor ^{-3.424}
Split phasing	5.256
Approach bus bay	1.309
Cycle facilities	0.706
Presence of right-turn lane	1.585
Rear-end crash (peak period & small intersection)	
Total AADT entering the intersection from the approach	factor ^{0.252}
Split phasing	5.256
Rear-end crash (off-peak period & large intersection)	
total AADT entering the intersection from the approach	factor ^{0.985}
Number of approach lanes	exp(.459×factor)
Left-turn storage length	(1+factor) ^{-1.142}
Lost time	factor ^{-1.739}
High speed	0.985
Standard phasing on approach	1.053
Cycle facilities	1.257
Free right-turn lane	1.227

Commercial	0.819
<hr/>	
Rear-end crash (peak period & large intersection)	
<hr/>	
total AADT entering the intersection from the approach	$\text{factor}^{1.181}$
Number of approach lanes	$\exp(.465 \times \text{factor})$
Left-turn storage length	$(1 + \text{factor})^{-1.478}$
High speed	1.756
Standard phasing on approach	1.257
Cycle facilities	0.443
Free right-turn lane	0.788
Commercial	0.925
<hr/>	
Rear-end crash (off-peak period & median intersection)	
<hr/>	
total AADT entering the intersection from the approach	$\text{factor}^{.496}$
Number of approach lanes	$\exp(.243 \times \text{factor})$
Lost time	$\text{factor}^{-0.209}$
Cycle facilities	0.753
Standard phasing on approach	0.637
Free right-turn lane	1.442
High speed	1.449
Approach bus bay	0.908
Commercial	0.9
<hr/>	
Rear-end crash (peak period & median intersection)	
<hr/>	
total AADT entering the intersection from the approach	$\text{factor}^{0.457}$
Number of approach lanes	$\exp(.277 \times \text{factor})$
High speed	1.63
Standard phasing on approach	0.572
Cycle facilities	0.754
Approach bus bay	0.692
Free right-turn lane	1.604
Commercial	0.653
<hr/>	
Loss-of-control crashes	
<hr/>	
total AADT entering the intersection from the approach	$\text{factor}^{0.541}$
Number of approaching lanes	$\exp(.144 \times \text{factor})$
Cycle length	$\text{factor}^{-0.704}$
Degree of saturation	$\text{factor}^{0.447}$

Residential	0.75
Split phasing	2.47
Upstream parking	0.58
Exit merge	1.47
Free right-lane turn	1.17
High speed	1.57
Approach bus bay	1.6
<hr/>	
Other crashes	
<hr/>	
total AADT entering the intersection from the approach	factor ^{0.262}
approaching width	factor ^{0.027}
Cycle time	factor ^{0.354}
Free right-lane turn	1.16
Coordinated	0.71
Shared turns	1.26
Split phasing	1.21
Advanced detector	0.44
High speed	1.98
Approach bus bay	1.27
Upstream parking	0.7
Exit merge	0.65
Commercial	1.83
<hr/>	

PART 2: IMPLEMENTATION OF CRASH PREDICTION AND MOBILITY MODELS INTO MULTIOBJECTIVE FUNCTIONS

This section contains an introduction to Genetic Algorithms (GA) and their application in the context of optimization of safety and mobility performance measures. It is organized into three subsections. In the first one, GA basic concepts are explained. The second subsection

describes the application of GA to similar problems, while the third provides a summary and recommendations regarding GA applications for the purposes of this study.

Genetic Algorithms Basic Concepts

GAs are adaptive methods which are widely used to solve search and optimization problems. GAs use a direct analogy of natural behavior. They work with a population of “individuals”, each representing a possible solution to a given problem. Each individual is assigned a “fitness score” according to how good a solution it produces to the problem. The most highly fitted individuals are given opportunities to “reproduce”, by cross breeding with other highly fitted individuals in the population. This produces new individuals as “offspring”, which share some features of their “parents”. The least fitted members of the population are less likely to be selected for reproduction, thus are weeded out gradually (14). In the GA, there are three important mechanisms: reproduction (selection), crossover, and mutation as shown in Figure 1.

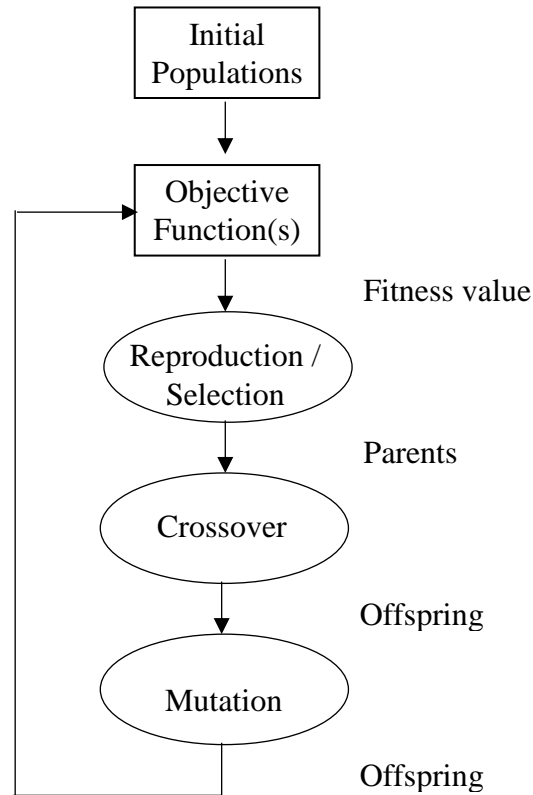


Figure 1: Scheme of Genetic Algorithm

The reproduction selects individuals with higher fitness value. Crossover takes two individuals, and cuts their chromosome strings (parameter set of the solution) at some randomly chosen positions, to produce offspring. Thus offspring inherit some genes (a specific parameter) from each parent. If crossover is not applied, any offspring would be exactly the same as one of their parents. Crossover facilitates the exploration of new parts of the search space by combining different solutions. The probability of crossover is typically between 0.6 and 1.0, while some argue that the probability should be between 0.4 and 0.9 (15). Mutation is applied to each child individually after crossover. It randomly alters each gene with a small probability P_m . Typically, P_m is 0.001, but Coley (15) argues that correcting a setting should be based on the specific problem. Many researchers have used $P_m \approx 1/L$, while others are concerned that $P_m \approx 1/(N\sqrt{L})$ and L is the length of solution strings.

The algorithm stops when results converge. Typically, the newest fitness value converges to the mean of all previous results.

A typical multiobjective function can be formulated as:

$$\begin{aligned} \text{Min} \quad & f(\mathbf{x}) = \{f_1(\mathbf{x}), f_2(\mathbf{x}), \dots, f_m(\mathbf{x})\} \\ \text{Subject to: } & \mathbf{x} \in D \text{ and } D = \{\mathbf{x}: g_y(\mathbf{x}) \leq 0, y = 1, 2, \dots, Y; h_z(\mathbf{x}) = 0, z = 1, 2, \dots, Z\} \end{aligned} \quad (7)$$

where \mathbf{x} is the parameter vector, and $f_i(\mathbf{x})$ is the i^{th} objective function among the total of m objective functions. $g_y(\mathbf{x})$ is the y^{th} inequality constraints among a total of Y inequality constraints and $h_z(\mathbf{x})$ is the z^{th} equality constraint among a total of Z equality constraints.

Signal Control Optimization

Azar S. et. al. (16) developed an algorithm of multiobjective design optimization with GA, called interactive sequential hybrid optimization technique (I-SHOT). The algorithm can convert problems with multiple objective functions into those with a single objective function without any modification in the typical GA procedures:

$$\text{Min} \sum_{i=1}^m w_i \left[\frac{f_i(\mathbf{x}) - \varepsilon_{i,good}}{\varepsilon_{i,bad} - \varepsilon_{i,good}} \right] \quad (8)$$

$$\text{Subject to: } f_i(\mathbf{x}) \leq \varepsilon_i, \quad i = 1, 2, \dots, m \quad \mathbf{x} \in D$$

where: $\varepsilon_i \in [\varepsilon_{i,good}, \varepsilon_{i,bad}]$ and $\varepsilon_{i,good}$ and $\varepsilon_{i,bad}$ are the good and bad values for the objective function I, or they can be understood as the maximum and minimum value of the objective function. They are used to scale each of the objectives in order to compare them on a fair level.

w_i is the weighting factor and can be calculated as:

$$w_i = \begin{cases} W_i + \frac{(1-\bar{W})}{\bar{W}} W_i & \text{if } \bar{W} > 1 \\ W_i & \text{if } \bar{W} = 1 \\ W_i + \frac{(1-\bar{W})}{(m-\bar{W})} (1 - W_i) & \text{if } \bar{W} < 1 \end{cases} \quad (9)$$

$$W_i = \text{random}(0,1) \forall i = 1, 2, \dots, m \text{ and } W = \sum_{i=1}^m W_i = 1$$

The procedures of the I-SHOT algorithm are the same as a typical GA in general.

However, decision makers should determine the following parameters before the first/each iteration: 1) the value of $\varepsilon_{i,bad}$ and $\varepsilon_{i,good}$ at the first iteration and the number of Pareto solutions to be generated; 2) weight vectors for Equation (8). The interactions continue until the decision maker is satisfied with the solution set.

Stevanovic et. al. (9) focus on single timing optimization based on delay and number of stops by VISSIM. They combined the two performance measures into a single objective function as:

$$\text{Performance Index} = \sum_i d_i + \frac{w}{3600} \sum_i s_i \quad (10)$$

where d_i and s_i are the delay and number of stops for each vehicle i , which completes its trip in the network during the simulation periods; w is the weight given to each stop (most optimization programs assign a w value of 10).

Yang et al. (17) also apply the weighted coefficient method to solve a multi-objective signal timing model. The goal of their study was to minimize performance measures including average delay, stop rate, and maximization of the traffic throughput. The fitness function is:

$$\text{Max Perf Index} = k_1 \times \left(1 - \frac{\text{avg}D}{\text{avg}D_{TRRL}}\right) + k_2 \times \left(1 - \frac{\text{avg}H}{\text{avg}H_{TRRL}}\right) + k_3 \times \left(\frac{Q}{Q_{TRRL}} - 1\right) \quad (11)$$

where: $\text{avg}D$ and $\text{avg}H$ = revised Webster delay and stop rate;

$\text{avg}D_{TRRL}$, $\text{avg}H_{TRRL}$, and Q_{TRRL} = revised Webster delay, Webster stop rate, and throughput under Webster timing scheme respectively;

Q = traffic throughput;

k_i = weighted coefficient of delay, stop rate, and traffic throughput, with adaptive adjustment by traffic demand variation to meet the optimization objectives of different traffic conditions; it can be calculated as:

$$U_1 = \frac{1-Y}{X}, U_2 = 1 - Y, U_3 = \frac{X}{1-Y}, k_i = \frac{U_i}{\sum_i^3 U_i} \quad (12)$$

where Y = total flow rate of intersections;

X = total saturation of intersections; and

U_1 = temporary weights of index I.

Summary and Conclusion

The studies identified have converted a multi-objective problem into a problem of a single objective function. In all of them, the typical Genetic Algorithm (GA) could be applied. Both Stevanovic's (9) and Yang's (17) formulas are straightforward, but neither one is easily applicable for our purposes. The goal of this project is to minimize delay (or number of stops) and crash frequency; however, it is challenging to scale these variables into compatible units and thus include in the same fitness function. Yang's method uses the ratio of each performance measure to the value calculated by the standard manual to scale the different measurements and include them into the same equation. However, for crash frequency, a standard manual does not exist. The methodology proposed by Azar S. et. al. (16) is preferred to the other two because: 1) it can convert problems of multi-objective functions into problems of single objective function without modifying the GA procedure; 2) the conversion procedure weights each objective function on an even level; 3) it can be applied to problems with a combination of discrete and continuous variables.

PART 3: SENSITIVITY ANALYSIS

Although the inputs for the safety models that are used in this work are known, the magnitude of the effect of each input for different scenarios is unknown. To hierarchize the degree of importance of each input of the model and determine which variables need to be calibrated, sensitivity analysis is recommended (30). Sensitivity analysis examines to what extent the outputs of a model depend on its inputs, by measuring the variation of the results as a function of different sources (31). Also, it helps identify interactions between two or more variables of the model (32).

Different classes of sensitivity analysis methods exist for different purposes (33). Local sensitivity analysis methods are used to identify trends for a specific variable within a determined sample space, while global sensitivity analysis considers the entire population.

In this work, the minimum number of variables and scenarios that are necessary to cover all the studied range, as described later in this report, would result in 8.1×10^7 simulations, which would be infeasible for the available computational resources. When this situation exists, screening methods are recommended (33).

The most known screening method is the classical *Ceteris Paribus*, in which one factor is varied through a range, with all other variables held constant. A statistically significant sample is calculated for the number of scenarios to be constructed. However, since only one variable is changed at a time, this simple method has limitations regarding the identification of interactions between variables and restrictions in terms of possible scenarios.

To remedy this situation, an evolution to the *Ceteris Paribus* concept has been proposed: the Factorial Effect Method (34,35). This method has been successfully applied to other transportation engineering studies (36). It was initially proposed by Morris (34) and further

developed in later studies (35) based on the concept of factorial effects – $d_i(x)$, that are defined individually for each input i until k of the model and is measured analogously to the price elasticities as:

$$d_i(x) = \frac{[y(x + e_i) - y(x)]}{\Delta_i} \quad (13)$$

where x = vectors of variables within the sample space;

Δ = Vector with the variation of all inputs i ; and

e_i = vector of zeros, with the value of Δ_i for the component i .

The sampling procedure consists of assembling an input matrix in a procedure called “trajectory” generation. The first row of the matrix reflects an initial vector of inputs, generally corresponding to a base scenario. The second row (vector x_1) is defined by changing only one of the variables by Δ_i . Likewise, the third row of the matrix (x_2) is constructed by varying another variable of x_1 . This is done successively, never changing the same variables twice, until all inputs have been varied. The order in which each variable is changed is random for each trajectory, so that no two matrices are the same. A trajectory z of a hypothetical model with three variables can be represented mathematically as:

$$z = \begin{vmatrix} x_1 & x_2 & x_3 \\ x_1 & x_2 + \Delta_2 & x_3 \\ x_1 + \Delta_1 & x_2 + \Delta_2 & x_3 \\ x_1 + \Delta_1 & x_2 + \Delta_2 & x_3 + \Delta_3 \end{vmatrix} \quad (14)$$

Note that for each trajectory, each factor is tested only once. In order to have statistically significant results, multiple trajectories have to be constructed. From the experience in other

studies (35), a minimum of 10 trajectories is sufficient for a reliable analysis, while more than 30 trajectories wouldn't add much more confidence to the results (37).

When all vectors from all trajectories are simulated, the factorial effects – $d_i(x)$ of all variables are compiled, forming the distribution F_i . The absolute values of $d_i(x)$ are also assembled, forming the G_i distribution. Based on those distributions, the following sensitivity measures are calculated for each variable i :

$$\mu_i = \sum_{j=1}^r \frac{d_{i,j}}{r} \quad (15)$$

$$\sigma_i = \sqrt{\sum_{j=1}^r \frac{(d_{i,j} - \mu_i)^2}{r}} \quad (16)$$

$$\mu_i^* = \sum_{j=1}^r \frac{|d_{i,j}|}{r} \quad (17)$$

where $d_{i,j}$ = factorial effect of the variable i as calculated in the trajectory j ; and

r = number of trajectories.

CHAPTER 3: METHODOLOGY

As described previously, Turner's crash prediction models (24) and the delay/stop equation in the HCS were used as the objective functions. The HCS incorporates the TRANSYT-7F optimization engine, which is based on hill-climbing and GA. Azar's I-SHOT GA (27) was used to convert the two objective functions into one single function. The weights for each objective function w_i in Equation 27 were set as user-determined instead of randomly generated.

Figure 2 summarizes the structure of the methodology, which was implemented in the HCS. A series of testing scenarios were established, comprising a base condition and variations to each input that might affect the outcome of the proposed method. At the end of each simulation, performance measures were obtained: (1) delays, to describe operation performance; (2) number of predicted crashes, to describe safety; and (3) gases, to quantify emissions.

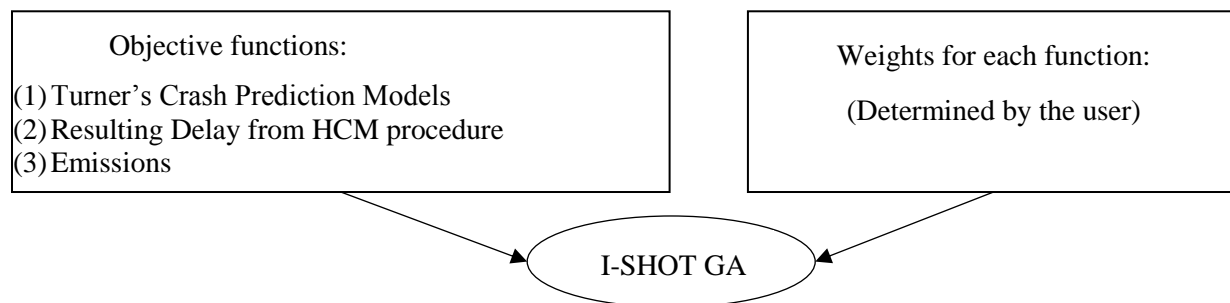


Figure 2: Methodology

The methodology and respective calculations were next implemented in the HCS – Streets. The following subsections describe the inputs into the HCS, the calculations performed, and the outputs obtained from the HCS.

New or Modified Inputs

A new set of inputs were required to apply the proposed method, accounting for safety, emissions, and delay simultaneously. Existing inputs were also used as variables to the new models. The new and the existing variables and described below, along with the respective HCS screen.

A. Primary Input Data screen (Figure 3):

- a. Demand: Demand affects delay and several other performance measures. The higher the demand, the higher is delay, emissions and crash probabilities. Also, the movement distribution (turning percentages) might play a role not only for operation performance, but also in safety analysis, since different types of crashes are associated with specific turning or through flows.
- b. Intersection Spacing: This variable represents the length of the segments from one intersection to another. This directly affects delay calculation and emissions, and might indirectly influence the overall safety.
- c. Lane configuration: It relates to the number of lanes and movement configuration, including the use of exclusive lanes or shared movements. This affects many of the variables that interrelate operations, emissions and safety.
- d. Left-turn pockets: Traditionally used to reduce delay and queuing, pockets are also associated with safety.
- e. Presence of free right-turn on red for motor vehicles (Y/N). This safety variable is defined by the existing input “RTOR”. If any value greater than zero is used, it is assumed that RTOR is permitted. This is a case where a trade-off is expected

between operations and safety. The use of RTOR has been found to improve operations, albeit at the cost of higher risks to traffic and pedestrians (24).

- f. Posted speed: As shown previously in this report, high speed has been associated with higher crash rates. On the other hand, the use of inappropriate speeds may also lead to inefficient operation, indirectly affecting safety and emission levels as well.
- g. Timing parameters: Cycle length, yellow time and all red directly affect total lost time, which in the proposed model might increase not only delay, but also emissions and some crash types, particularly rear-end crashes.
- h. Phasing: Regarding phasing, higher risks associated with permitted left-turning may be compensated by the greater efficiency this strategy allows. Depending on the demand levels and other intersection characteristics, it is possible to experience improvements in all three performance measures.

PRIMARY INPUT DATA

General

Urban Street: TestBed
 Intersection: Int 3
 Description:
 Forward Direction: EB Area Type: CBD
 Segment Length, ft: 700 Duration: 0.25
 All Segment Lengths PHF: 0.92

Traffic

	EBL	EBT	EBR	WBL	WBT	WBR	NBL	NBT	NBR	SBL	SBT	SBR
Demand, veh/h	104	483	104	180	840	180	30	140	30	30	140	30
Lane Width, ft	12.0	12.0	12.0	12.0	12.0	12.0	12.0	12.0	12.0	12.0	12.0	12.0
Storage Length, ft	400	700	0	400	1000	0	0	1000	0	0	1000	0
Saturation, pc/h/ln	1900	1900	1900	1900	1900	1900	1900	1900	1900	1900	1900	1900
Heavy Vehicles, %	0	0	0	0	0	0	0	0	0	0	0	0
Grade, %	0	0	0	0	0	0	0	0	0	0	0	0
Buses, per h	0	0	0	0	0	0	0	0	0	0	0	0
Parking, per h	0	N	0	0	L	0	0	N	0	0	N	0
Bicycles, per h	0	0	0	0	0	0	0	0	0	0	0	0
Pedestrians, per h	130	0	0	100	0	0	200	0	0	140	0	0
Arrival Type	3	3	3	3	3	3	3	3	3	3	3	3
Upstream Filtering (I)	I-EB	0.96	I-WB	1.00	I-NB	1.00	I-SB	1.00				
Initial Queue, veh	0	0	0	0	0	0	0	0	0	0	0	0
Speed Limit, mi/h	35	35	35	35	35	35	30	30	30	30	30	30
Detector, ft	40	40	40	40	40	40	40	40	40	40	40	40
RTOR, veh/h	0	0	0	0	0	0	0	0	0	0	0	0
Unsignalized Move...	<input type="checkbox"/>	<input type="checkbox"/>	<input type="checkbox"/>	<input type="checkbox"/>	<input type="checkbox"/>	<input type="checkbox"/>	<input type="checkbox"/>	<input type="checkbox"/>	<input type="checkbox"/>	<input type="checkbox"/>	<input type="checkbox"/>	<input type="checkbox"/>
Unsignalized Delay	0.0	0.0	0.0	0.0	0.0	0.0	0.0	0.0	0.0	0.0	0.0	0.0

Phasing

Cycle, s: 95
 Pre-Timed Signal:
 Offset, s: 24
 Phase 2 Direction: EB
 Phase 4 Direction: SB
 Reference Phase: 2
 Reference Point: End
 Force Mode: Fixed
 Side Street Split Phasing:
 Uncoordinated Intersection:
 Field-Measured Phase Times:

Phase Duration

	EBL	EBT	WBL	WBT	NBL	NBT	SBL	SBT
Green	69.8	13.2	0.0	0.0	0.0	0.0	0.0	0.0
Yellow	3.0	3.0	0.0	0.0	0.0	0.0	0.0	0.0
Red	3.0	3.0	0.0	0.0	0.0	0.0	0.0	0.0

Timing

	EBL	EBT	WBL	WBT	NBL	NBT	SBL	SBT
Assigned Phase	(2)		(6)		(8)		(4)	
Phase Split, s	0.0	55.0	0.0	55.0	0.0	40.0	0.0	40.0
Yellow Change, s	4.0	3.0	4.0	3.0	4.0	3.0	4.0	3.0
Red Clearance, s	0.0	3.0	0.0	3.0	0.0	3.0	0.0	3.0
Minimum Green, s	6	6	6	6	6	6	6	6
Lag Phase	<input type="checkbox"/> EL <input type="checkbox"/> ET <input type="checkbox"/> WL <input type="checkbox"/> WT <input type="checkbox"/> NL <input type="checkbox"/> NT <input type="checkbox"/> SL <input type="checkbox"/> ST							
Passage Time, s	2.0	2.0	2.0	2.0	2.0	2.0	2.0	2.0
Recall Mode	Min	Min	Off	Mir	Off	Off	Off	Off
Dual Entry	<input type="checkbox"/> EL <input checked="" type="checkbox"/> ET <input type="checkbox"/> WL <input checked="" type="checkbox"/> WT <input type="checkbox"/> NL <input checked="" type="checkbox"/> NT <input type="checkbox"/> SL <input checked="" type="checkbox"/> ST							
Dallas Phasing	<input type="checkbox"/> EW <input type="checkbox"/> N/S	Simultaneous Gap		<input checked="" type="checkbox"/> EW <input checked="" type="checkbox"/> N/S				

Figure 3: HCS Primary Input Data Screen

- B. Additional factors for the Detailed Input / Full Optimization screen (Figure 4):
- The objective functions in the current version of the HCS are: 1) percent base FFS; 2) travel time; 3) travel speed; 4) arterial stops; 5) arterial delay; 6) overall delay. In this project, additional optimization options are added to allow for combined consideration of mobility (delay), safety (crashes) and emissions (grams of gases). The default option is overall delay;
 - When the multi-objective function is selected, there is a box showing the current optimum performance measures of the last simulation, if already defined.

Figure 4: HCS Detailed Input Data / Full Optimization Screen for the Arterial

C. Safety and Emissions Details screen (Figure 6)

A new screen was created to include parameters that affect only safety calculations. This interface can be accessed through the “Safety and Emissions” button placed on Full Optimization / Detailed Inputs screen. It allows the calculation and verification of the safety and emissions values that are expected for the current set of inputs. Also, this screen houses safety inputs, as follows:

- a. Intersection depth, per direction. The intersection depth defines the distance to be covered by an approaching vehicle for reaching the opposite approach. It is measured as the distance between the stop bar on the subject approach arm and the beginning of the downstream through intersection leg. This variable affects intersection size, which influences the probability of many types of crashes, particularly rear-end accidents. Intersection size can be classified as:

- i. Small: those with an intersection depth of 82 ft (25 m) or less, usually having 1 or 2 lanes per approach;
 - ii. Medium: those having an intersection depth between 82 ft and 131 ft and 2 lanes per approach; and
 - iii. Large: those having an intersection depth of 131 ft (40m) or greater with 3 or more lanes for at least two of their approaches.
- b. Land use. Some Highway Capacity Manual (HCM) default values change for Central Business District (CBD) areas. Also, some safety models differentiate between CBD and residential areas. In the HCS interface, if the option “Other” is selected on the Main Input screen, as opposed to CBD, there is an option to specify it as “Residential” on the Safety and Emission screen.
- c. Presence of Mast arm signal display (Y/N), that affects the prediction model for right angle crashes. Figure 5 defines the signal display classified as the mast arm display.

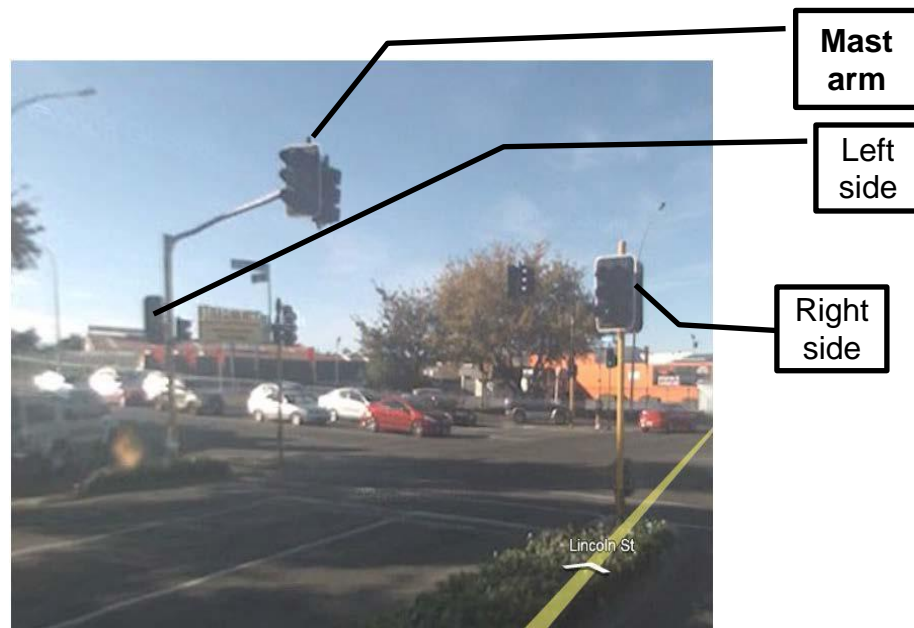


Figure 5. Types and Location of Signal Display

- d. Presence of median island that can be used by pedestrians (Y/N).
- e. Presence of merge on exit side (Y/N): this variable reflects the situation where the road width decreases due to lane drops, blockages, incidents or road works. If, at the Main Input screen, the number of lanes decrease between intersections, this variable is automatically set as Y.
- f. Presence of bicycle facilities, including bike lane only, shared bicycle and vehicle lane or bicycle storage areas at the approaches (Y/N).
- g. Presence of parking areas 328 ft (100 m) of stop bar (Y/N).
- h. Presence of upstream bus bay within 328 ft (100 m) of stop bar (Y/N).
- i. Weights given to each performance measure within the calculation of the GA objective function. The default value for each one is set as: $1/\text{number of objectives}$. For example, if delay and safety are selected, the default values of

weights are 0.5 and 0.5; if delay, safety, and emissions are selected, the default values of weights are 0.33, 0.33, and 0.33.

Intersection Data		East-West		North-South			
Intersection Depth		110		110			
Residential Area Use	<input checked="" type="checkbox"/>						
		EB	WB	NB	SB		
Presence of Mast Arm Signal Display	<input checked="" type="checkbox"/>	<input checked="" type="checkbox"/>	<input checked="" type="checkbox"/>	<input checked="" type="checkbox"/>	<input checked="" type="checkbox"/>		
Presence of Median Island	<input type="checkbox"/>	<input type="checkbox"/>	<input type="checkbox"/>	<input type="checkbox"/>	<input type="checkbox"/>		
Presence of Merge on exit side	<input checked="" type="checkbox"/>	<input checked="" type="checkbox"/>	<input type="checkbox"/>	<input type="checkbox"/>	<input type="checkbox"/>		
Multimodal Input Data		EB	WB	NB	SB		
Presence of Bicycle Facilities	<input type="checkbox"/>	<input type="checkbox"/>	<input type="checkbox"/>	<input type="checkbox"/>	<input type="checkbox"/>		
Presence of Upstream Bus Bay within 330 feet from stop bar	<input checked="" type="checkbox"/>	<input checked="" type="checkbox"/>	<input checked="" type="checkbox"/>	<input checked="" type="checkbox"/>	<input checked="" type="checkbox"/>		
Presence of Upstream Parking within 330 feet from stop bar	<input type="checkbox"/>	<input type="checkbox"/>	<input type="checkbox"/>	<input type="checkbox"/>	<input type="checkbox"/>		
Calculation Data							
K, %		15.0					
Optimization Data		Delay, %		Safety, %		Emissions, %	
Weights, %		50.0		25.0		25.0	

Figure 6: Safety and Emissions Screen

Optimization Procedures

The optimization procedures provided by the HCS were applied, comprising the following basic steps:

- 1) Optimization of the cycle length using hill-climb search technique;
- 2) Optimization of the phasing sequence and offsets simultaneously, using GA; and
- 3) Optimization of the splits and offsets using GA.

The HCS procedures first determine the optimal cycle length followed by the optimal phasing and splits. This process cannot guarantee that the cycle length is still optimal after the change of splits. Moreover, though the hill-climbing technique is sometimes faster than the GA, results obtained from this method highly depend on initial populations (seeds), which may not be reliable. In other word, it cannot guarantee that results represent the global optimum. Therefore, another test procedure was conducted and compared with the results produced by the HCS. The final proposed procedure is as follows:

- 1) Optimization of the cycle, split, and offset simultaneously using GA; and
- 2) Optimization of the phasing sequence, split, and offsets simultaneously using GA.

Objective Function

If the optimization is focused on operational analysis only the traditional objective function implemented in HCS-Streets can be used. The performance measures that can be chosen are: (a) Percent Base FFS, (b) Travel Time, (c) Travel Speed, (d) Arterial Stops, (e) Arterial Delay, (f) Overall Delay, or (g) Balanced Delay.

If the optimization is focused on both mobility and safety, then the objective function will use the combination of delay and number of stops as well as safety prediction functions as follows:

$$\text{Min} \left(w_{\text{delay}} \frac{f_{\text{delay}}(x) - \varepsilon_{\text{delay,good}}}{\varepsilon_{\text{delay,bad}} - \varepsilon_{\text{delay,good}}} + w_{\text{safety}} \frac{f_{\text{safety}}(x) - \varepsilon_{\text{safety,good}}}{\varepsilon_{\text{safety,bad}} - \varepsilon_{\text{safety,good}}} \right) \quad (18)$$

where w_{delay} and w_{safety} are the weights to be used for overall delay and number of crashes in the objective function. The defaults are 0.5. These may be modified by the user in the “Safety and Emissions Details” input data screen.

$\epsilon_{delay,good}$ is the minimum value for the overall delay function;

$\epsilon_{delay,bad}$ is the maximum value for the delay function;

$\epsilon_{safety,good}$ is the minimum value for the safety function; and

$\epsilon_{safety,bad}$ is the maximum value for the safety function.

Note that “good” and “bad” values for each variable correspond to upper and lower boundaries of each output; these are needed to normalize the values of three different performance measures so that optimization can consider all of them simultaneously.

The $f_{safety}(x)$ reflects the total number of crashes over a five-year period for the arterial, calculated as the sum of all types of crashes. For each type, there is a crash prediction model that is structured as a function of traffic and “crash modification factors” (CMF), independent multiplicative factors that reflect the effect of geometry or control conditions different from base conditions for which the model as initially calibrated.

If the optimization focuses on mobility and emissions, then the objective function will use the combination of delay/number of stops and emission prediction functions as follows:

$$\text{Min} \left(w_{delay} \frac{f_{delay}(x) - \epsilon_{delay,good}}{\epsilon_{delay,bad} - \epsilon_{delay,good}} + w_{emission} \frac{f_{emission}(x) - \epsilon_{emission,good}}{\epsilon_{emission,bad} - \epsilon_{emission,good}} \right) \quad (19)$$

where w_{delay} and $w_{emission}$ are the weights to be used for delay and emissions in the objective function. The defaults are 0.5, and they may be modified by the user in the “Safety and Emissions Details” input data screen.

$\varepsilon_{delay,good}$ is the minimum value for the delay function;

$\varepsilon_{delay,bad}$ is the maximum value for the delay function;

$\varepsilon_{emission,good}$ is the minimum value for the emission function; and

$\varepsilon_{emission,bad}$ is the maximum value for the emission function.

Finally, if the optimization addresses all three areas (mobility, safety, and emissions), then the objective function will use the combination of delay, safety, and emission prediction functions as follows:

$$\text{Min} \left(w_{delay} \frac{f_{delay}(x) - \varepsilon_{delay,good}}{\varepsilon_{delay,bad} - \varepsilon_{delay,good}} + w_{safety} \frac{f_{safety}(x) - \varepsilon_{safety,good}}{\varepsilon_{safety,bad} - \varepsilon_{safety,good}} + w_{emission} \frac{f_{emission}(x) - \varepsilon_{emission,good}}{\varepsilon_{emission,bad} - \varepsilon_{emission,good}} \right) \quad (20)$$

where w_{delay} , w_{safety} , and $w_{emission}$ are the weights to be used for delay, safety and emissions in the objective function, respectively. The defaults are 1/3 for each, and may be modified by the user in the “Safety and Emissions Details” input data screen.

The following subsections describe the calculation of each component of these objective functions.

Operations

The operations component is calculated in terms of delay, as follows:

$$d(x) = d_1 + d_2 + d_3 \quad (21)$$

$$d_1 = \frac{c[1-(g/c)]^2}{2[1-(\frac{g}{c}) \times \min(1, X)]} \quad (22)$$

$$d_2 = 900T \left\{ (X - 1) + \sqrt{(x - 1)^2 + \frac{8k \times I \times X}{c_A \times T}} \right\} \quad (23)$$

$$d_3 = \frac{3600}{vT} \left(t_A \frac{Q_b + Q_e - Q_{eo}}{2} + \frac{Q_e^2 - Q_{eo}^2}{2c_A} - \frac{Q_b^2}{2c_A} \right) \quad (24)$$

where: d = control delay (sec/veh);

d_1 = uniform delay (sec/veh);

d_2 = incremental delay (sec/veh);

d_3 = initial queue delay (sec/veh);

C = cycle length (sec);

g = effective green time for the lane group (sec);

v = traffic flow per hour (veh/h);

c_A = average capacity for the lane group (veh/h);

X = volume/capacity ratio for the subject lane group = v/c_A ;

T = duration of analysis period (h);

I = upstream filtering factor;

Q_b = initial queue at the start of the analysis period (veh / h);

t_A = adjusted duration of unmet demand in the analysis period (h);

Q_e = queue at the end of the analysis period (veh);

Q_{eo} = queue at the end of the analysis period when $v \geq c_A$ and $Q_b = 0.0$ (veh); and

k = incremental delay factor, related to actuated control (0.4 to 0.5, being 0.5

recommended for pre-timed phases)

Safety

The safety component is calculated by adding the number of predicted crashes of several types:

$$A_{Total} = A_{right-angle} + A_{left-turn-against} + A_{rear-end} + A_{loss\ of\ control} + A_{other} \quad (25)$$

Each crash type is estimated by a different submodel, as a function of AADT and varying CMFs. In HCS-Streets, the user defines hourly flow for each traffic direction independently. The AADT is calculated by dividing the hourly volumes by a user defined K factor. The default value for K is 0.1.

Most crash prediction models use the total $AADT$ for each approach as an input. Two of them, however ($A_{right-angle}$ and $A_{left-turn-against}$), use movements volumes. The equations presented in this report take as a reference the northbound movement, with each movement coded as shown in Figure 7.

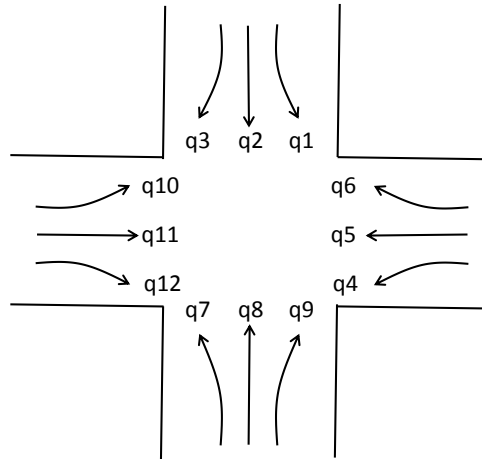


Figure 7. Signalized intersection movement codes (Reference: northbound direction)

$A_{Right-angle}$ is total number of predicted right angle crashes in five years, estimated as:

$$A_{right-angle} = b_0 \times q_8^{0.311} (q_5 + q_{11})^{0.362} \times e^{0.356N} \times I_D^{0.602} \times C^{0.037} \times AR^{-0.636} \times F_{split\ phasing} \times F_{mast} \times F_{coordinated} \times F_{detector} \times F_{shared\ turns} \times F_{isle} \quad (26)$$

Table 6 provides definitions and the parameters to be used in this equation.

Table 6. Right-angle crash (all day)

Factors	Symbol	Coefficient
constant	b_0	2.08×10^{-5} to 1.54×10^{-4}
daily volume of through vehicles on movement 2	q_2	$q_2^{0.311}$
daily volume of through traffic coming from left side + daily volume of through traffic coming from right side	$q_5 + q_{11}$	$(q_5 + q_{11})^{0.362}$
Number of approaching lanes	N	$\exp(0.356 \times N)$
Intersection depth	I_D	$I_D^{0.602}$
Cycle length	C	$C^{0.037}$
All-red time	AR	$AR^{-0.636}$
Split phasing on the approach	$F_{split\ phasing}$	0.69
Presence of mast-arm display	F_{mast}	0.74
Signal coordination with the upstream intersection	$F_{coordinated}$	1.31
Presence of advanced detector	$F_{detector}$	2.06
Shared-turns	$F_{shared\ turns}$	1.19
Presence of raised median/central island on the approach	F_{isle}	0.67

$A_{left-turn-against}$ is the total number of left turn crashes in five years and is estimated as

follows:

$$A_{left-turn-against} = b_0 \times q_7^{0.155} \times (1 + L_{LT})^{-0.124} \times e^{0.352N_T} \times X_{LT}^{0.397} \times C^{-0.683} \times F_{LT\ protection} \times F_{shared\ turns} \times F_{isle} \times F_{bike} \quad (27)$$

Table 7 provides the parameters to be used in this equation,

Table 7. Left-turn-against crash (all day)

Factors	Symbol	Coefficient
constant	b_0	2.27 to 4.41
daily volume of left-turning vehicles on movement 7	q_7	$q_7^{0.155}$
Left-turn storage length	L_{LT}	$(1 + L_{LT})^{-0.124}$
Number of through lanes	N_T	$\exp(0.352 \times N_T)$
Degree of saturation for left turn movement	X_{LT}	$X_{LT}^{0.397}$
Cycle length	C	$C^{-0.683}$
Fully protected left-turn in the phasing	$F_{LT\ protection}$	0.71
Shared left-turn/through lane present on the approach	$F_{shared\ LT}$	0.72
Presence of raised median/central island on the approach	F_{isle}	1.22
Presence of cycle lanes or storage on the approach	F_{bike}	1.35

$A_{rear-end}$ is the total number of rear-end crashes in five years, and depends on the intersections size:

- Small: those having an intersection depth of 82 ft or less;
- Large: those having an intersection depth of 131 ft or greater; and
- Medium: those not lying in either of the two above categories

For these three categories, $A_{rear-end}$ is estimated as follows:

$$A_{rear-end, small} = b_0 \times q^{0.447} \times (1 + L_{LT})^{-0.259} \times L_C^{-3.424} \times F_{split\ phasing} \times F_{bus} \times F_{bike} \times F_{FRT} \quad (28)$$

$$A_{rear-end, (medium)} = b_0 \times q^{0.496} \times e^{0.243N} \times L_C^{0.209} \times F_{bike} \times F_{std\ phasing} \times F_{FRT} \times F_{high\ speed} \times F_{bus} \times F_{CBD} \quad (29)$$

$$A_{rear-end, (large)} = b_0 \times q^{0.356} \times e^{0.459N} \times (1 + L_{LT})^{-1.142} \times L_C^{-1.739} \times F_{bike} \times F_{std\ phasing} \times F_{FRT} \times F_{high\ speed} \times F_{CBD} \quad (30)$$

Table 8 provides the parameters to be used in these equations.

Table 8. Rear-end crashes (all day, for all sizes of intersections)

Factors	Symbol	Coefficient		
		Small	Medium	Large
Constant	b_0	0.658 to 7.95	1.14×10^{-3}	0.774 to 3.92
total AADT entering the intersection from the approach	Q	0.447	0.496	0.356
Number of approaching lanes	N	0	0.243	0.459
Left-turn storage length	L_{LT}	-0.259	0	-1.142
Lost time ($Y + AR + \text{Green Extension}$)	L_C	-3.424	0.209	-1.739
Split phasing on the approach	$F_{split\ phasing}$	5.256	1	1
Standard phasing on approach	$F_{std\ phasing}$	1	0.637	1.053
Presence of free-right-turn lane for motor vehicles	F_{FRT}	1.585	1.442	1.227
Presence of cycle lanes or storage on the approach	F_{bike}	0.706	0.753	1.257
Speed limit of 50 mph (80kph) or more on the approach	$F_{high\ speed}$	11	1.449	0.985
Upstream bus bay within 328 ft (100 m) of limit line	F_{bus}	1.309	0.908	1
Area is CBD	F_{CBD}	1	0.9	0.819

$A_{loss-of\ control}$ is the total number of loss-of-control crashes in five years, and is estimated as follows:

$$A_{loss\ of\ control} = b_0 \times q^{0.541} \times e^{0.144N} \times C^{-0.704} \times X^{0.447} \times F_{residential} \times F_{split\ phasing} \times F_{park} \times F_{exit\ merge} \times F_{FRT} \times F_{high\ speed} \times F_{bus} \quad (31)$$

Table 9 provides the parameters to be used in this equation.

Table 9. Loss-of-control crashes

Factor	Symbol	Coefficient
Constant	b_0	0.111 to 9.12x10 ⁻²
total AADT entering the intersection from the approach	q	$q^{0.541}$
Number of approaching lanes	N	$\exp(.144 \times N)$
Cycle length	C	$C^{-.704}$
Degree of saturation	X	$X^{0.447}$
Area land use is residential	$F_{residential}$	0.75
Split phasing on the approach	$F_{split\ phasing}$	2.47
Presence of upstream parking within 328 ft (100m) of limit line	F_{park}	0.58
Merge present on exit side	$F_{exit\ merge}$	1.47
Presence of free-right-turn lane for motor vehicles	F_{FRT}	1.17
Speed limit of 50 mph (80kph) or more on the approach	$F_{high\ speed}$	1.57
Presence of upstream bus bay within 328 ft (100 m) of limit line	F_{bus}	1.6

A_{other} is the total number of other crashes in five years and is estimated as follows:

$$A_{other} = b_0 \times q^{0.262} \times W^{0.027} \times C^{0.354} \times F_{FRT} \times F_{coordinated} \times F_{shared\ turns} \times F_{split\ phasing} \times F_{adv\ detector} \times F_{high\ speed} \times F_{bus} \times F_{park} \times F_{exit\ merge} \times F_{CBD} \quad (32)$$

Table 10 provides the parameters to be used in this equation.

Table 10. Other crashes

Factor	Symbol	Coefficient
Constant	b_0	1.55×10^{-3} to 2.38×10^{-3}
total AADT entering the intersection from the approach	q	$q^{0.262}$
approaching width	W	$W^{0.027}$
Cycle length	C	$C^{0.354}$
Presence of free-right-turn lane for motor vehicles	F_{FRT}	1.16
Signal coordination with the upstream intersection	$F_{coordinated}$	0.71
Lanes with shared movements (left-turn/through, right-turn/through, or both present on the approach	$F_{shared\ turns}$	1.26
Split phasing on the approach	$F_{split\ phasing}$	1.21
Presence of advanced detector(s) on the approach	$F_{adv\ detector}$	0.44
Speed limit of 50 mph (80kph) or more on the approach	$F_{high\ speed}$	1.98
Presence of upstream bus bay within 328 ft (100 m) of limit line	F_{bus}	1.27
Presence of upstream parking within 328 ft (100m) of limit line	F_{park}	0.7
Merge present on exit side	$F_{exit\ merge}$	0.65
Area is CBD	F_{CBD}	1.83

To validate the results implemented in the HCS for the safety component, a spreadsheet was built, containing all equations and tables shown in this section. Figure 8 and Figure 9, show the input/calculation screen and the output of the spreadsheet respectively, which considers one intersection at a time. After several rounds of testing, all results produced by the HCS and the spreadsheet were identical, confirming the accuracy of the implementation of the model.

Hourly Volumes		Approach			Unit	Category																														
		East-West		North-South																																
<table border="1"> <tr><td>q_1</td><td>180</td><td>q_2</td><td>250</td><td>q_3</td><td>50</td></tr> <tr><td>q_{12}</td><td>80</td><td colspan="3" rowspan="3"> </td><td>q_4</td><td>200</td></tr> <tr><td>q_{11}</td><td>1145</td><td>q_5</td><td>1145</td></tr> <tr><td>q_{10}</td><td>200</td><td>q_6</td><td>80</td></tr> <tr><td colspan="2"></td><td>q_9</td><td>50</td><td>q_8</td><td>250</td><td>q_7</td><td>180</td></tr> </table>		q_1	180	q_2	250	q_3	50	q_{12}	80				q_4	200	q_{11}	1145	q_5	1145	q_{10}	200	q_6	80			q_9	50	q_8	250	q_7	180	Intersection Depth (I_D)	100	100	ft	Safety	
q_1	180	q_2	250	q_3	50																															
q_{12}	80				q_4	200																														
q_{11}	1145				q_5	1145																														
q_{10}	200				q_6	80																														
		q_9	50	q_8	250	q_7	180																													
<p>General Inputs</p> <p>Cycle Length (C) 70 s</p> <p>Coordination FALSE</p> <p>Split-Phasing FALSE</p> <p>Region Commercial</p> <p>K Factor (%) 10.0%</p> <p>Intersection Size Medium</p>		Lanes (N)	2	2	2	2	HCS (geometry)																													
<p>AADT</p> <table border="1"> <tr><td>q_1</td><td>1800</td><td>q_2</td><td>2500</td><td>q_3</td><td>500</td></tr> <tr><td>q_{12}</td><td>800</td><td colspan="3" rowspan="3"> </td><td>q_4</td><td>2000</td></tr> <tr><td>q_{11}</td><td>11450</td><td>q_5</td><td>11450</td></tr> <tr><td>q_{10}</td><td>2000</td><td>q_6</td><td>800</td></tr> <tr><td colspan="2"></td><td>q_9</td><td>500</td><td>q_8</td><td>2500</td><td>q_7</td><td>1800</td></tr> </table>		q_1	1800	q_2	2500	q_3	500	q_{12}	800				q_4	2000	q_{11}	11450	q_5	11450	q_{10}	2000	q_6	800			q_9	500	q_8	2500	q_7	1800	Number of Through Lanes (N_T)	2	2	2	2	HCS (geometry)
q_1	1800	q_2	2500	q_3	500																															
q_{12}	800				q_4	2000																														
q_{11}	11450				q_5	11450																														
q_{10}	2000				q_6	800																														
		q_9	500	q_8	2500	q_7	1800																													
		Shared Turns	TRUE	TRUE	TRUE	TRUE	HCS (geometry)																													
		Shared Left Turn	FALSE	FALSE	TRUE	TRUE	HCS (geometry)																													
		LT Storage	200	200	0	0	ft HCS (Traffic)																													
		Lane width	12	12	12	12	ft HCS (Traffic)																													
		Posted Speed	45	45	30	30	mi/h HCS (Traffic)																													
		Yellow (Y)	3	3	3	3	s HCS (phasing)																													
		All Red (AR)	2	2	2	2	s HCS (phasing)																													
		Full LT Protection	TRUE	TRUE	FALSE	FALSE	HCS (phasing)																													
		Start-up Lost Time (l_s)	2	2	2	2	s HCS (detailed)																													
		Green Extension (e)	2	2	2	2	s HCS (detailed)																													
		Free-right-turn (F_{RTT})	FALSE	FALSE	FALSE	FALSE	Safety																													
		Mast-Arm	TRUE	TRUE	TRUE	TRUE	Safety																													
		Median Island	TRUE	TRUE	FALSE	FALSE	Safety																													
		Advanced Detector	TRUE	TRUE	TRUE	TRUE	Safety																													
		Merge present on the exit side	FALSE	FALSE	FALSE	FALSE	Safety																													
		Bicycle facilities	FALSE	FALSE	FALSE	FALSE	Safety																													
		Bus bay within 330 ft from stop bar	FALSE	FALSE	FALSE	FALSE	ft Safety																													
		Parking within 330 ft from stop bar	FALSE	FALSE	FALSE	FALSE	ft Safety																													
		Degree of Saturation - Approach (X)	0.280	0.457	0.300	0.206	Aggregated results																													
		Degree of Saturation - Left Turn (X_{LT})	0.059	0.468	0.347	0.037	Movement group result																													
		Lost Time (L_c)	5	5	5	5	s HCS (internal)																													

Figure 8. Spreadsheet built to validate HCS implementation – Inputs and calculations

	Approach				Total
	EB	WB	NB	SB	
$A_{right-angle}$	0.38	0.38	0.61	0.61	1.97
$A_{left-turn-against}$	0.21	0.48	0.55	0.23	1.48
$A_{rear-end}$	0.17	0.17	0.10	0.10	0.54
$A_{loss-of-control}$	0.19	0.24	0.11	0.09	0.63
A_{other}	0.11	0.11	0.09	0.09	0.40
A_{total} (5 year)	1.07	1.38	1.46	1.12	5.02
$A_{average}$ (year)	0.21	0.28	0.29	0.22	1.00

Figure 9. Spreadsheet built to validate HCS implementation – Outputs

Emissions

The following emission estimation model has been developed based on NGSIM data (Part A of this report). The general function for emission estimation is:

$$Emission = B_1 * VMT + \frac{B_2}{average\ speed} + \frac{B_3 * number\ of\ stops}{average\ speed} \quad (33)$$

where B_1 , B_2 , and B_3 are coefficients of the independent variables. In summary, the best prediction models for various environmental measures are presented in the following equations:

$$CO(g) = 10.875 \times VMT + 3078.297 \times \frac{1}{avgspeed} + 1.470 \times \frac{NumStops}{avgspeed} \quad (34)$$

$$NO_x(g) = 1.241 \times VMT + 185.490 \times \frac{1}{avgspeed} + 0.206 \times \frac{NumStops}{avgspeed} \quad (35)$$

$$EC(joule) = 7.223 \times 10^6 \times VMT + 1.084 \times 10^9 \times \frac{1}{avgspeed} + 2.388 \times 10^6 \times \frac{NumStops}{avgspeed} \quad (36)$$

$$CO_2Equi(g) = 519.1 \times VMT + 77950.6 \times \frac{1}{avgspeed} + 171.6 \times \frac{NumStops}{avgspeed} \quad (37)$$

Note that the VMT is given in miles and the speed given in mph.

Main outputs

During each iteration, all performance measures used by the objective function are recorded, along with other parameters usually provided by the HCS. At the end of the procedure, the following main outputs are produced:

1. Optimized signal-timing plan;

2. Diagnostic messages, that comprise mostly warnings on input variables that might compromise the quality of the results;
3. Optimization Status: this comprises (a) information on the performance function, including the original, optimum and average values, as well as the % improvement throughout the run time; (b) and the Run Status, including the current generation number, the generation optimum and total time elapsed, in sec;
4. Performance measures for each component: delay (sec/veh), safety (total number of crashes), and emissions (total g of gases) for the optimized signal plan

Figure 10 shows the new output screen that was created for this project.

The screenshot displays the 'Full Optimization' window with the following sections:

- Input Parameters:**
 - Optimization:**
 - Include this Intersection in Optimization:
 - Objective Function: Delay & Safety & Er (dropdown)
 - Cycle Length: Safety and Emission
 - Splits:
 - Offsets:
 - Phasing Sequence:
 - Dallas Phasing:
 - Minimum Cycle, s: 60
 - Maximum Cycle, s: 160
 - Cycle Increment, s: 5
 - Master Intersection: 1
 - Forward Weighting, %: 50
 - Reverse Weighting, %: 50
 - Number of Generations: 200
 - Population Size: 10
 - Crossover Probability, %: 30
 - Mutation Probability, %: 4.0
 - Convergence Threshold, %: 0.010
 - Random Number Seed: 7781
- Optimization Status:** (collapsed)
- Diagnostic Messages:** (collapsed)
- Safety, Emission, Delay Values:**
 - Total Crashes, 5 Years: 21.8
 - Total Emissions: 2026.0 g
 - Overall Delay: 17.1 sec
- Controls:** Start (green), Info (yellow), Stop (red), Save, Cancel.

Figure 10. New Output Screen

CHAPTER 4: RESULTS

This chapter, provides the results obtained from HCS-Streets for a base scenario and the sensitivity analysis test scenarios. For each scenario, the following are calculated: expected total number of crashes, expected overall delay for the arterial (sec/veh) and emissions, measured in terms of total g of gases.

To identify and rank the input variables affecting the global fitness output and each performance measure, multiple runs are made using the new algorithm, varying key inputs in predetermined ranges. The sensitivity analysis method described in Chapter 2 is used and statistical tests are applied to the results at 95% confidence.

BASE SCENARIO

For the base scenario, a set of characteristics were assumed for each input type used by HCS, as described in the following subsections.

Design

A three-intersection arterial was designed for testing. All three intersections have the same configuration, as shown in Figure 11. The main street approaches have two lanes with a 200-ft exclusive left-turn pocket and a shared right and through lane. The side streets have two lanes: a shared left and through lane and a shared right and through lane. The link length between Intersection 1 and Intersection 2 as well as Intersection 2 and Intersection 3 is 1,300 feet. The length of all other links for both the main street and side streets are 1000 feet. Other characteristics are:

- The speed limit of the arterial is 45 mi/h and that of the side streets is 30 mi/h.;
- Lane width of 12 feet; and
- Zero grade on all approaches.

Demand

The arterial is in a CBD area. The base traffic demand for all the movements at each of the three intersections are as shown in Figure 11. This demand level was defined after a series of tests, so that the level of service at the arterial components ranged from C to E, leaving room for improvement, while avoiding spillbacks that would result from LOS F.

The K factor, which reflects the relationship between those hourly volumes, used by capacity and level of service calculations and the average annual daily traffic (AADT), used for crash estimation, was set as 10%.

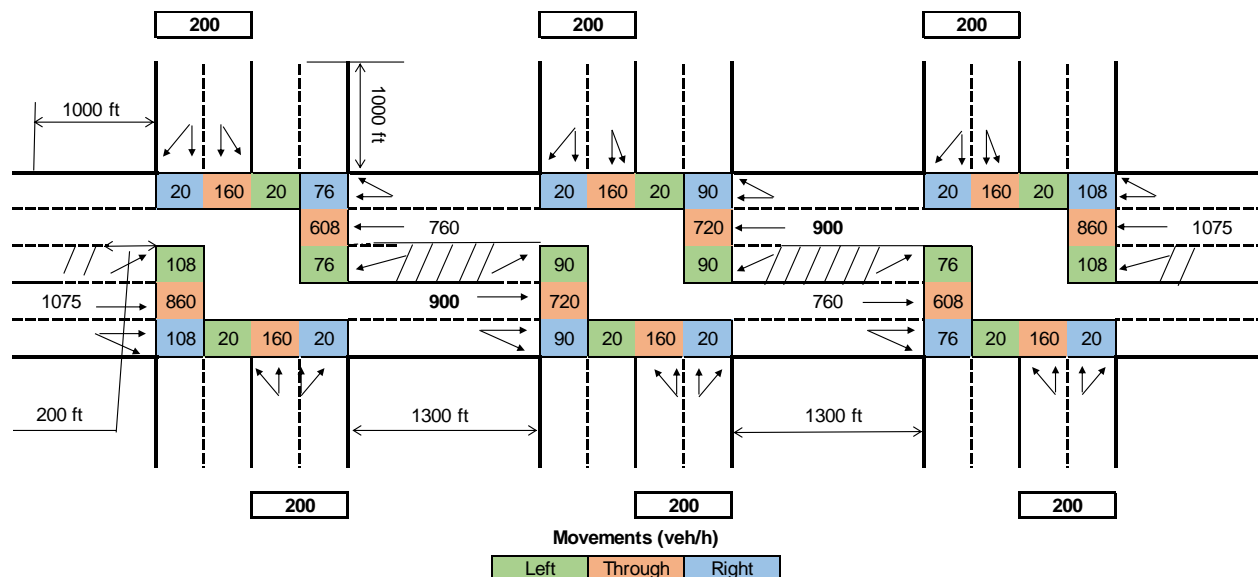


Figure 11: Configuration and Demand on Testing Arterial

Safety-only characteristics

The following characteristics have a direct effect only on the safety component of the model:

- Intersection depth of 110 feet (medium sized intersection);
- There are median islands along the arterial;
- There are mast arm signal displays at each intersection;
- Constant width along the arterial, (no merges on the exit sides);
- There is no parking along any of the links; and
- There are no bus bays or bicycle facilities present.

Other variables that affect safety include the degree of saturation X of each approach, the degree of saturation of the left turn lane groups and the lost time L_C . Those variables are calculated iteratively by HCS as intermediate results and used in the final model.


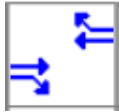


Control

For the control variables, the values used for the base scenario were:

- Coordinated arterial;
- All intersections have semi-actuated control and detectors are present at each side street approach and protected left turn movements;
- Minimum green of 6 sec;
- Yellow time fixed as 3 sec at every approach;
- Red clearance time set as 2 sec for all intersections;
- No RTOR;
-

- Exclusive left-turn phasing is used for the main street while permissive only left-turn phasing is used for the side streets, hence no split phasing is used for the side streets.
- The initial signal timing used in optimization assumed a cycle length of 120 sec, which is recommended by the 2010 HCM (p 18-78, Exhibit 18-33). The green duration is assumed to be proportional to the respective demands. In a preliminary optimization run performed with the proposed GA, the plan provided in Table 11 was obtained, with the use of a lag phase for westbound left movement and a total cycle length of 70 seconds.

Table 11. Initial Signal Timing Plan

Phasing Diagram				
Green (s)	7.0	19.6	4.8	13.0
Yellow (s)	3	3	3	3
Red Clearance (s)	2	2	2	2

Optimization guidelines

Figure 12 shows the Full Optimization screen, with the settings used for the project, as defined after rounds of preliminary testing. The selected objective function was “Delay & Safety & Emissions”, and all signal parameters were considered for optimization. Cycles between 60 and 160 sec were allowed, at 5 sec increment.

As recommended by HCS-Streets, for the GA, population sizes of 10 were used, with 30% crossover probability, a minimum 4.0% mutation probability, and 1% convergence

threshold. However, a maximum of 1,000 generations was permitted, as opposed to the 100 default value, to ensure convergence to the global solution.

Finally, regarding the weights given to each component of the objective function, a balanced 33%/33%/33% scheme was chosen for operations/safety/emissions, for the base scenario.

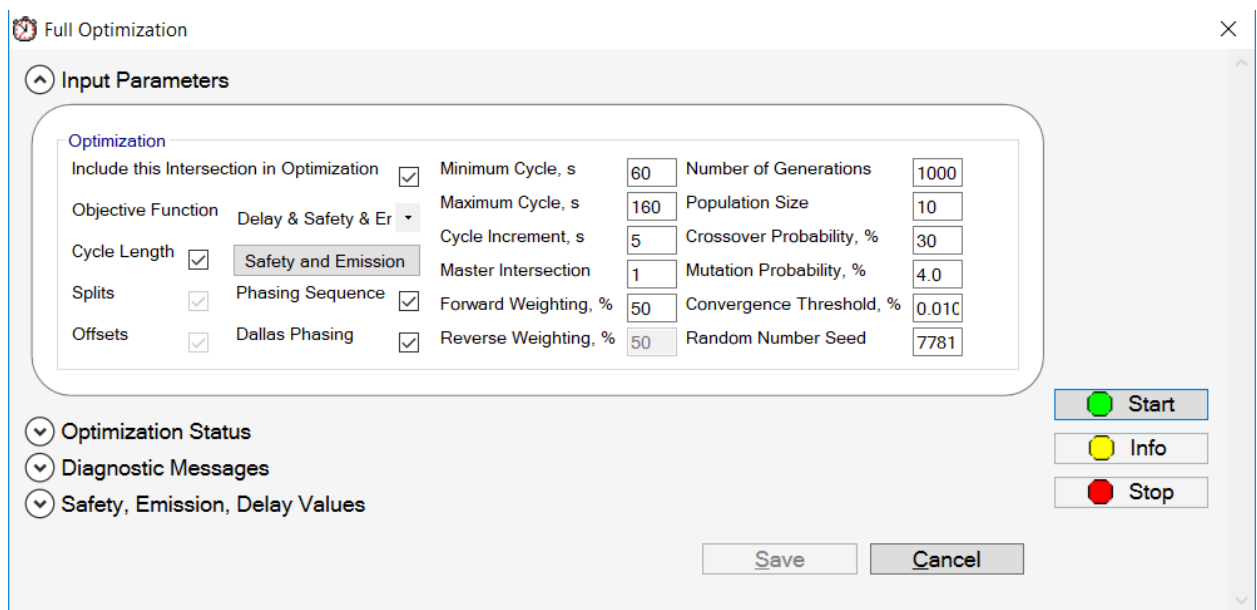


Figure 12: Configuration and Demand on Testing Arterial

SENSITIVITY ANALYSIS

Whereas the individual effect of each submodel used in this study is known, the outputs produced by their combined use through the HCS implementation must be explored and validated. This section implements the Factorial Sampling Method, described in Chapter 2, as follows:

1. Selection of key variables to be considered for a sensitivity analysis and variation range;
2. Set sensitivity analysis “trajectories”, defined by series of consecutive scenarios in which, for each simulation, one variable is varied within the predefined range while all other variables are kept as in the previous scenario;
3. Run the model implemented in HCS for each scenario of each trajectory;
4. Build a database with resulting performance measures (delay, crashes and emissions) and associated input data;
5. Analyze data; and
6. Perform statistical tests.

Variables

Variation to the model’s parameters were tested, within three main domains: (a) design; (b) demand; (c) control; (d) safety-only parameters; and (e) weights given to each optimization criterion. Three levels were considered per variable. The following items explain the variables that were tested and their levels of variation.

A. Intersection Spacing:

The initial distance between intersections was 1300 ft (base scenario). Another two levels of spacing were also tested, corresponding to 700 ft and 1900 ft. This variation affects not only coordination patterns, but storage areas as well.

B. Intersection Size:

Intersection size was defined by two variables: total number of lanes on the arterial and intersection depth. Also, the All Red time was affected by this parameter. The three levels were:

- Small Intersections: 2-lane arterial, 80 ft intersection depth and 1 sec all red;
- Medium Intersections (base scenario): 3-lane arterial, 110 ft intersection depth and 2 sec all red time; and
- Large Intersections: 4-lane arterial, 140 ft intersection depth and 3 sec all red time.

C. Left turn pocket:

In addition to the 200 ft. left-turn pocket of the base scenario, the analysis considered longer left-turn lanes (400 ft), and no pockets at all. Finally, when the leftmost lane is set as shared left and through movements, the pocket length considered by HCS equals the segment length, which can potentially affect the model.

D. Shared turns:

This comprises two different variables, for right and left turns:

- For right turns, it relates to the use of the rightmost lane for shared right and through movements. The default value is Yes (shared right turn present); and
- For left turns, it relates to the use of the leftmost lane for shared right and through movements. The default value is No (exclusive left-turn lane/pocket).

E. Arterial Posted Speed:

The posted speed in the base scenario was set as 45 mph. The other levels tested include a lower speed arterial (35 mph) and another with a 55 mph posted speed, which would be classified in the New Zealand model as a “high speed” arterial. The speeds at the minor streets were kept constant at 30 mph.

F. Volume Increments:

Volume multipliers of 0.9 and 0.8 were used to verify the sensitivity of the model to different traffic levels. These multipliers were applied to traffic flows entering from both the arterial and minor streets. As indicated earlier, oversaturated conditions were not considered in this study.

G. Turning Percentages:

The default turning percentage was 10% of the total flow at the central intersection and each minor street approach. Increments of 5% were also tested, from 5% to 15%. Separate tests were undertaken for right and left turns, for a total of 2 variables and 6 levels.

H. K Factor:

K factor varied from 5% to 15%. K in the base scenario was 10%. Note that the hourly volumes used for the delay calculation remain unchanged, and the K factor only affects the AADT estimation which is calculated for use by the safety models.

I. Protected Left:

In the base scenario, a protected phase exists for the main street. Depending on intermediate results for some scenarios, a permitted phase may also be suggested by HCS-Streets. However, when this variable is set as “No”, no protected phases are allowed.

J. Mast-arm Signal Display and Median Islands:

In the base scenario, this type of signal display is used for all approaches at each intersection, as well as median islands for pedestrian crossings. When set as “No”, mast-arm displays and islands are removed from the entire corridor.

K. Merge on Exit Side:

This variable reflects the reduction in the road width after the intersection is cleared, for each direction. As stated before, this may correspond to lane drops, incidents or road works. Due to HCM limitations in handling bottlenecks on urban streets, in this work, merges were considered solely as road width reductions from the intersection center to the roadway, that tend to affect the safety component of the model.

L. Bicycle Facilities, Parking and Bus Bays within 330 ft from Stop Bar:

The default for these variables was set as “No”, Alternatively, the influence of each of these elements was examined with respect to intersection safety.

M. Weight sensitivity

Three sets of scenarios were established for weight testing: operations, safety and emissions. For each, the 33/33/33 weights were changed to one of the following schemes: One variable dominance (50/25/25, 25/50/25 or 25/25/50, depending on the tested domain); or two variable dominance (40/40/20, 40/20/40 or 20/40/40).

Summary of Tested Variables and Ranges

Table 12 lists all variables included in the sensitivity analysis. For each variable, the table shows the three levels and full range considered, along with the respective units.

The highlighted values reflect the inputs used in the base scenario.

Table 12. Variables Included in the Sensitivity Analysis and Variation Range

Domain	N°	Variable	Unit	Levels			Range
				1	2	3	
Design	1	Intersection spacing	feet	700	1300	1900	1200
	2	Size (Number of total lanes on arterial) ¹		2	3	4	2
	3	Left turn pockets	feet	0	200	400	400
	4	Shared right turn		No	Yes		
	5	Shared left turn		No	Yes		
	6	Arterial Posted Speed	mph	35	45	55	10
Demand	7	Volume increments (multipliers)	veh/h/ln	0.8	0.9	1	0.2
	8	Right turn percentages	%	5%	10%	15%	0.1
	9	Left turn percentages	%	5%	10%	15%	0.1
	10	K factor	%	5%	10%	15%	0.1
Control	11	Protected Left		No	Yes		
Safety factors	12	Mast-arm signal display		No	Yes		
	13	Median island		No	Yes		
	14	Merge on exit side		No	Yes		
	15	Bicycle facilities		No	Yes		
	16	Bus bay within 330 feet from stop bar		No	Yes		
	17	Parking within 330 feet from stop bar		No	Yes		
	18	Area type is residential		No	Yes		
Weight	19	Operations		33/33/33	50/25/25	40/40/20	25
	20	Safety	%	33/33/33	25/50/25	20/40/40	25
	21	Emissions		33/33/33	25/25/50	40/20/40	25

Method

The application of the Factorial Sampling Method is based on the construction of trajectories, with input vectors randomly generated. Each trajectory allows for the measurement of the effect of each factor to each performance measure.

The trajectory is composed of vectors of input data. Since there are 21 variables of interest, each trajectory is represented by a matrix with 21 columns (variables) and 22 rows, in which the first row reflects the base scenario and all other rows represent variations of each variable within one of the levels, as shown in Table 12. Table 13 was developed to generate

random trajectories. From the base scenario (first row), each consecutive vector is composed by varying one single input, as highlighted, to one of the three possible levels. The selected levels and the order in which the variables are assorted are defined randomly.

Table 13. Random Trajectory Generator

	Intersection spacing	Size	Left turn pockets	Shared right turn	Shared left turn	Arterial Posted Speed	Volume increments (multipliers)	Right turn percentages	Left turn percentages	K factor	Protected Left	Mast-arm signal display	median island	Merge on exit side	Bicycle facilities	Bus bay 330 feet from stop bar	Parking 330 feet from stop bar	Area type is residential	Operations	Safety	Emissions	
INITIAL VECTOR	2	2	2	2	1	2	3	2	2	2	2	2	2	1	1	1	1	1	1	1	1	1
median island	2	2	2	2	1	2	3	2	2	2	2	2	1	1	1	1	1	1	1	1	1	1
K factor	2	2	2	2	1	2	3	2	2	1	2	2	1	1	1	1	1	1	1	1	1	1
Left turn percentages	2	2	2	2	1	2	3	2	3	1	2	2	1	1	1	1	1	1	1	1	1	1
Merge on exit side	2	2	2	2	1	2	3	2	3	1	2	2	1	2	1	1	1	1	1	1	1	1
Right turn percentages	2	2	2	2	1	2	3	1	3	1	2	2	1	2	1	1	1	1	1	1	1	1
Shared right turn	2	2	2	1	1	2	3	1	3	1	2	2	1	2	1	1	1	1	1	1	1	1
Mast-arm signal display	2	2	2	1	1	2	3	1	3	1	2	1	1	2	1	1	1	1	1	1	1	1
Bicycle facilities	2	2	2	1	1	2	3	1	3	1	2	1	1	2	1	1	1	1	1	1	1	1
Arterial Posted Speed	2	2	2	1	1	3	3	1	3	1	2	1	1	2	2	1	1	1	1	1	1	1
Intersection spacing	3	2	2	1	1	3	3	1	3	1	2	1	1	2	2	1	1	1	1	1	1	1
Volume increments (multipliers)	3	2	2	1	1	3	2	1	3	1	2	1	1	2	2	1	1	1	1	1	1	1
Bus bay 330 feet from stop bar	3	2	2	1	1	3	2	1	3	1	2	1	1	2	2	2	1	1	1	1	1	1
Safety	3	2	2	1	1	3	2	1	3	1	2	1	1	2	2	2	1	1	1	1	2	1
Protected Left	3	2	2	1	1	3	2	1	3	1	1	1	1	2	2	2	1	1	1	2	1	1
Shared left turn	3	2	2	1	2	3	2	1	3	1	1	1	1	2	2	2	1	1	1	2	1	1
Left turn pockets	3	2	3	1	2	3	2	1	3	1	1	1	1	2	2	2	1	1	1	2	1	1
Area type is residential	3	2	3	1	2	3	2	1	3	1	1	1	1	2	2	2	1	2	1	2	1	1
Parking 330 feet from stop bar	3	2	3	1	2	3	2	1	3	1	1	1	1	2	2	2	2	2	1	2	1	1
Emissions	3	2	3	1	2	3	2	1	3	1	1	1	1	2	2	2	2	2	1	2	2	1
Size	3	1	3	1	2	3	2	1	3	1	1	1	1	2	2	2	2	2	1	2	2	2
Operations	3	1	3	1	2	3	2	1	3	1	1	1	1	2	2	2	2	2	2	2	2	2

Each scenario (vector) is run in HCS-Streets, by constructing an input file using the real values that correspond to the levels determined in Table 13 and listed in Table 12. The resulting performance measures are then registered in another spreadsheet, and the factorial effect of each variable is calculated as:

$$d_{i,j}(x) = \frac{MOE(x_k) - MOE(x_{k-1})}{\Delta} \quad (38)$$

where: $d_{i,j}(x)$ = factorial effect of the factor i of trajectory j ;

$MOE()$ = performance measure for a given vector;

x_k = input data vector for row k ;

Δ = Variation of the tested variable between vector x_k and x_{k-1} .

Three statistics are calculated: the average of the factorial effects across all trajectories (μ); the average of the absolute factorial effects (μ^*); and the standard deviation (σ). The higher the μ^* , the higher the indication that a variable has a significant impact on the performance measure analyzed.

A fourth measure β was calculated as the relationship between the modulus of μ and μ^* :

$$\beta_i = \frac{|\mu_i|}{\mu_i^*} \quad (39)$$

The closer this factor is to zero, the greater the indication that the sign of the factorial effect is dependent on the overall scenario. A factor of 1 means that the variable always affects the output in the same way.

Data Analysis

The following paragraphs show the results of the sensitivity analysis on each performance measure – delay, crashes and emissions. The results were obtained from a total of 10 trajectories.

A. Operations:

Table 14 ranks all variables by the average of the factorial effects across all trajectories (μ). A positive sign indicates a positive relationship between the variable and the performance measure. For instance, a certain increase in the demand (volume multipliers) is associated with an average increase of 2.5 in delay for the solution area of this experiment.

In the case of binary variables, the “yes” value is associated with 1. As an example, it can be stated that the use of a protected left phase as opposed to permitted movements increased the delay at a rate of 6.9, on average, for the studied case. In this case, a safer solution leads to poorer operations, and the tradeoffs between the two aspects must be carefully analyzed.

Variables with a negative sign, on the other hand, on the average, improve operations. This was true for shared movements and specially for the intersection size. As expected, the more the number of lanes, the better is the operational performance.

The β values, as stated previously, indicate how much the results depend on the other variables. The closer to zero, the higher the variability of the sign of μ . An example of this is the “Intersection Spacing”: although longer spacing was found to decrease delays in many instances by providing more storage area, in some cases it merely translated in a greater length to be cleared by traffic and less efficient coordination. The results were very much linked to through flows and the percent of turning movements.

Table 14. Ranking of μ for All Variables and Associated β – Delay

Variable	μ	β
Protected Left	6.920	1.000
Volume increments (multipliers)	2.510	1.000
Left turn percentages	1.020	1.000
Safety	0.545	0.947
Right turn percentages	0.500	0.610
Mast-arm signal display	0.190	1.000
Arterial Posted Speed	0.140	0.438
Median island	0.120	1.000
K factor	0.120	0.750
Bicycle facilities	0.030	1.000
Bus bay within 330 feet from stop bar	0.001	1.000
Parking within 330 feet from stop bar	0	0
Merge on exit side	-0.020	1.000
Emissions	-0.156	0.204
Left turn pockets	-0.280	0.467
Intersection spacing	-0.280	0.269
Operations	-0.925	1.000
Area type is residential	-1.230	0.953
Shared right turn	-3.369	1.000
Shared left turn	-3.410	1.000
Size	-12.540	0.997

To better illustrate this variability on the results across multiple scenarios, Figure 13 provides box-plots that represent the variability of the factorial effects for each variable, allowing for better comparison between them. As shown, larger intersection sizes always lead to less delay, although the variability for this effect is rather high. On the other extreme, higher volume increments result in higher delay, with very low variability.

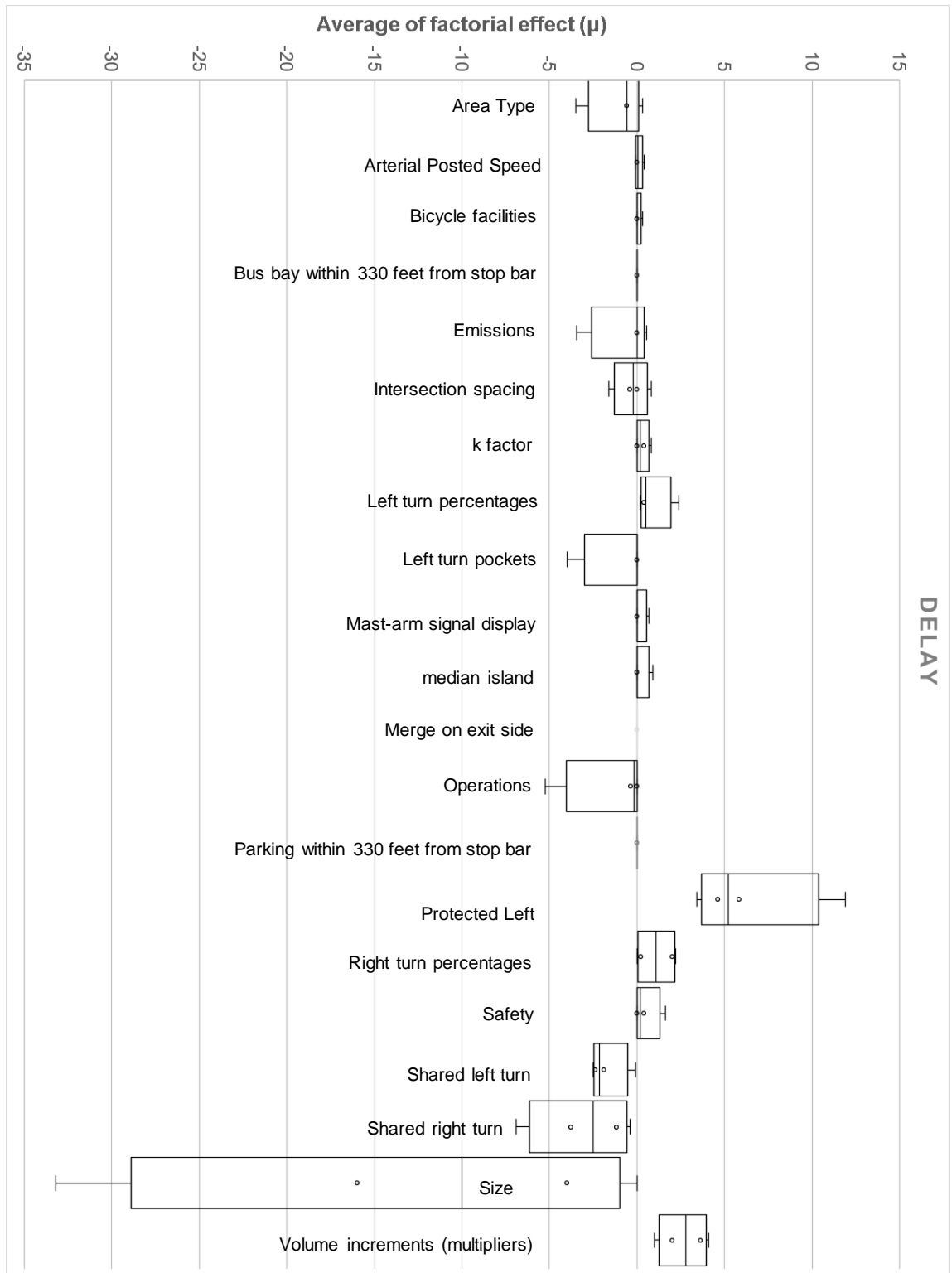


Figure 13: Variability of μ for each variable – Delay

Table 15 presents the average of the absolute factorial effects (μ^*) of each variable, which is considered the most statistically significant measure in the method used, ranked from the highest impact to the least. The table also shows the standard deviation associated with each one and the confidence interval, at the 95% confidence level.

Table 15. Ranking and Confidence Interval of μ^* for All Variables – Delay

Variable	Lower Bound	μ^*	Upper Bound	Std. Dev σ
Size	3.037	12.580	22.123	15.397
Protected Left	4.464	6.920	9.376	3.963
Shared left turn	1.166	3.410	5.654	3.621
Shared right turn	2.098	3.369	4.640	2.051
Volume increments (multipliers)	1.538	2.510	3.482	1.569
Area type is residential	0.647	1.290	1.933	1.037
Intersection spacing	0.282	1.040	1.798	1.223
Left turn percentages	0.371	1.020	1.669	1.048
Operations	-0.113	0.925	1.963	1.675
Right turn percentages	0.143	0.820	1.497	1.092
Emissions	-0.019	0.768	1.555	1.270
Left turn pockets	-0.275	0.600	1.475	1.412
Safety	0.152	0.575	0.999	0.683
Arterial Posted Speed	0.065	0.320	0.575	0.412
Mast-arm signal display	-0.003	0.190	0.383	0.311
K factor	-0.017	0.160	0.337	0.286
Median island	-0.060	0.120	0.300	0.290
Bicycle facilities	-0.029	0.030	0.089	0.095
Merge on exit side	-0.006	0.020	0.046	0.042
Bus bay within 330 feet from stop bar	-0.001	0.001	0.003	0.003
Parking within 330 feet from stop bar	---		---	

Although the ranking shown in Table 15 provides some insight on the magnitude of the impact of each variable, the confidence intervals and standard deviations suggest that one-to-one comparisons of variables with similar effects is not straightforward. For that reason, a multiple pairwise comparison statistical test was performed.

In a preliminary analysis, it was noted that the distribution of μ^* didn't follow a normal (Gaussian) pattern. For that reason, the non-parametric Kruskal Wallis test was chosen, which accounts for the frequency that each variable assumes a specific position in the overall ranking.

The results are shown in Table 16. The much higher value of H as compared to the critical Chi indicates that H_0 can be rejected, and at least two variables differ from each other. To specify which ones, multiple pairwise comparisons were made, as illustrated by the Tukey lines, on the right side of Table 16.

Each line stretches from a specific variable (from 1 to 8 in this case) until the variables that could not be considered statistically different from the base (H_0 can't be reject). For example, Protected Left, that was taken in the preliminary analysis as the most important variable in terms of impact on mobility, can only be considered statistically different, and thus more relevant, than the variable "Emissions".

Likewise, "Volume Increments" can be considered more relevant than the length of left turn pockets, but its impact on delays is not necessarily higher than that caused by right or left turn percentages.

It can be concluded that, while some variables are notably more significant (especially the use of protected lefts, shared turns, intersection size, and volumes), others highly depend on other variables and the corresponding test scenario.

Table 16. Kruskal Wallis Test – Delay

Multiple comparisons (pairwise)				KRUSKALL-WALLIS TABLE							
				Chi	16.92						
				H	121.63						
				Tukey Line from Variable <i>n</i>							
T	T ² / <i>n</i>	Variable	\bar{R}	1	2	3	4	5	6	7	8
1619	261954	Protected Left	194.6								
1946	378497	Shared right turn	173.4								
1607	258245	Volume increments (multipliers)	165.0								
1734	300502	Size	161.9								
1650	272250	Shared left turn	160.7								
1421	201782	Area type is residential	142.1								
1327	175960	Intersection spacing	132.7								
1253	157001	Left turn percentages	125.3								
979	95746	Right turn percentages	114.2								
1142	130302	Emissions	98.7								
987	97318	Operations	97.9								
748	55876	Arterial Posted Speed	97.2								
960	92160	Safety	96.0								
972	94478	Left turn pockets	74.8								
673	45293	K factor	68.8								
688	47266	Mast-arm signal display	67.3								
578	33408	Median island	57.8								
484	23426	Merge on exit side	51.0								
510	26010	Bicycle facilities	48.4								
462	21344	Bus bay 330 feet from stop bar	46.2								
420	17640	Parking 330 feet from stop bar	42.0								

B. Safety:

Similarly to Table 14, Table 17 ranks all variables by their effect on the predicted number of crashes, as measured by the factor μ and corresponding β . Large intersections are associated with a much higher number of crashes, especially angle and rear-end crashes. However, this was true only when no pockets for left turns were present. When this is the case, the use of shared left turns could mitigate the risk factors, as reflected by the μ for this variable.

Other relevant variables were demand-related (volumes and K factor) and the use of shared right turns.

Table 17. Ranking of μ for All Variables and Associated β – Safety

Variable	μ	β
Size	31.940	0.946
Volume increments (multipliers)	3.660	1.000
Shared right turn	3.360	1.000
Bus bay within 330 feet from stop bar	2.160	1.000
Left turn percentages	0.940	0.855
Merge on exit side	0.760	1.000
Intersection spacing	0.580	0.547
Operations	0.568	1.000
Bicycle facilities	0.450	0.652
Arterial Posted Speed	0.090	0.134
Emissions	-0.004	0.008
Safety	-0.422	0.905
Protected Left	-0.470	0.376
Right turn percentages	-0.620	0.756
Area type is residential	-0.810	0.730
Mast-arm signal display	-1.850	1.000
Parking within 330 feet from stop bar	-1.950	1.000
Median island	-2.720	1.000
Left turn pockets	-3.560	0.908
K factor	-9.580	1.000
Shared left turn	-15.570	0.919

Figure 14 graphically shows those results, and illustrates the variability of the Shared Left Turn and Size variables. As stated previously, this happens because a large increase in the number of predicted crashes occurs only when a large intersection has no pockets or shared left turn lanes. Higher K factors consistently decrease crashes, as they are associated with lower AADTs, while higher volumes would increase exposure and crashes.

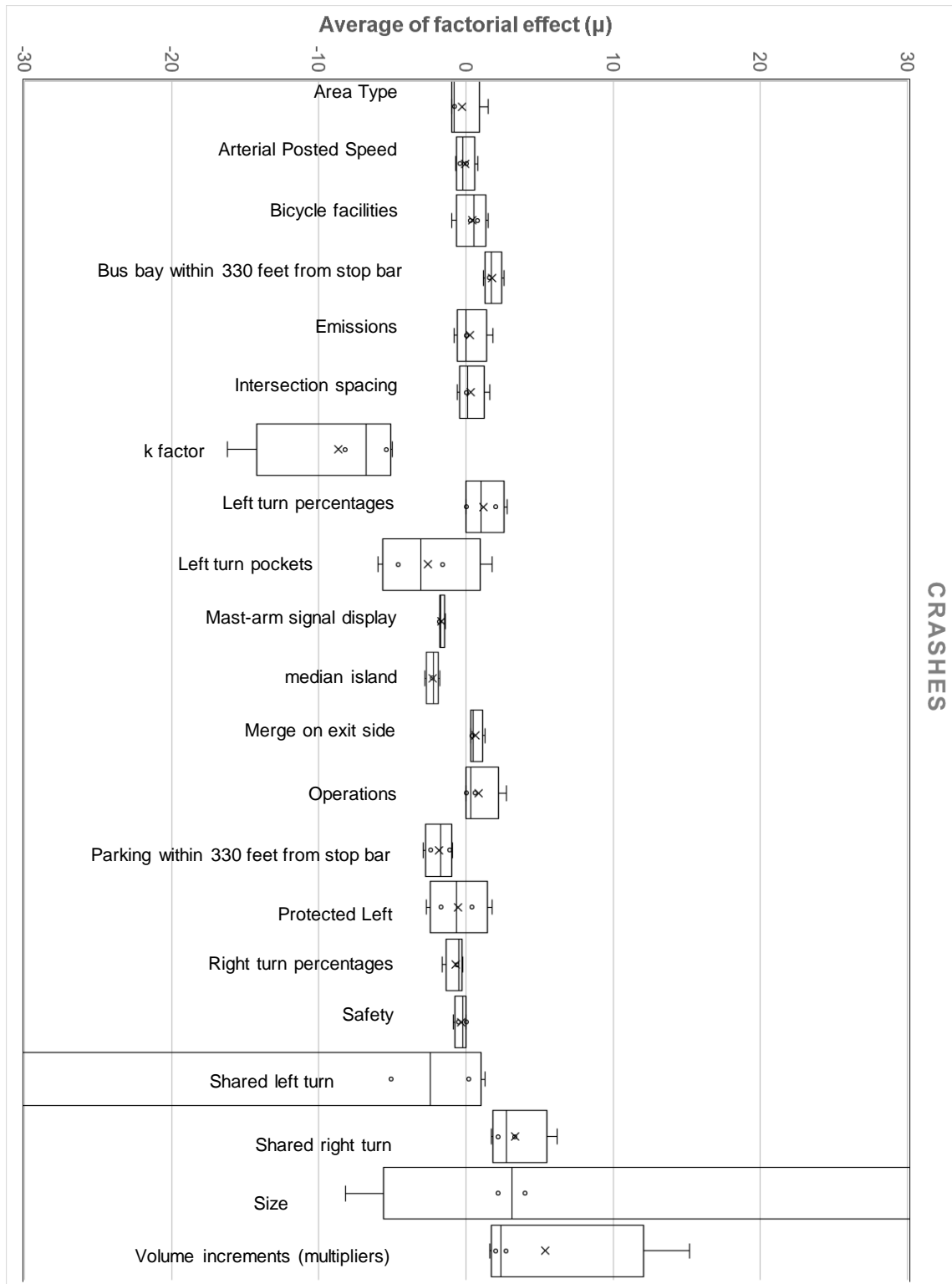


Figure 14: Variability of μ for each variable – Crashes

Table 18 and Table 19 present the confidence interval and ranking of μ^* for all variables regarding safety, and the corresponding Kruskal Wallis tests, respectively. Note that β values shown in Table 17 were closer to 1 as compared to the operations analysis, indicating that the factorial effects on safety have constant signs for most variables. As a result, the magnitude of μ^* values shown on Table 18 are similar to the μ values, and the same variables are the most important to the model: Size, Shared Turns, K factor, Pockets and Volume Increments.

Table 18. Ranking and Confidence Interval of μ^* for All Variables – Safety

Variable	Lower Bound	μ^*	Upper Bound	Std. Dev σ
Size	-27.422	33.780	94.982	98.745
Shared left turn	-11.877	16.950	45.777	46.510
K factor	6.555	9.580	12.605	4.880
Left turn pockets	1.366	3.920	6.474	4.121
Volume increments (multipliers)	1.117	3.660	6.203	4.102
Shared right turn	2.386	3.360	4.334	1.572
Median island	2.100	2.720	3.340	1.000
Bus bay within 330 feet from stop bar	1.490	2.160	2.830	1.081
Parking within 330 feet from stop bar	1.548	1.950	2.352	0.649
Mast-arm signal display	1.542	1.850	2.158	0.497
Protected Left	0.342	1.250	2.158	1.464
Area type is residential	0.555	1.110	1.665	0.895
Left turn percentages	0.368	1.100	1.832	1.182
Intersection spacing	0.297	1.060	1.823	1.231
Right turn percentages	0.362	0.820	1.278	0.739
Merge on exit side	0.537	0.760	0.983	0.360
Bicycle facilities	0.241	0.690	1.139	0.725
Arterial Posted Speed	0.022	0.670	1.318	1.046
Operations	0.048	0.568	1.088	0.839
Emissions	-0.018	0.518	1.053	0.865
Safety	0.123	0.467	0.811	0.555

Kruskal Wallis tests (Table 19) had similar results with the ones observed for the operations analysis. Statistically significant differences can be established for variables with up

to 10 levels of difference in the ranking, but never for consecutive variables, for the given sample size and confidence level. The K factor was the variable found to differ the most, while the weight variables, labeled as “Operations”, “Safety” and “Emissions”, barely influenced the outcomes.

Table 19. Kruskal Wallis Test – Safety

Multiple comparisons (pairwise)				KRUSKAL-WALLIS TABLE									
				Chi	16.92								
				H	119.14								
				Tukey Lines									
T	T ² /n	Variable	R̄	1	2	3	4	5	6	7	8	9	10
1465	214476	K factor	199.7										
1127	127013	Shared right turn	166.5										
1997	398801	Median island	157.4										
1508	227406	Volume increments (multipliers)	156.5										
1565	244923	Left turn pockets	150.8										
1665	277223	Size	146.5										
1574	247590	Parking 330 feet from stop bar	134.7										
1345	180903	Bus bay 330 feet from stop bar	134.5										
1347	181306	Mast-arm signal display	130.0										
1300	168870	Shared left turn	112.7										
927	85840	Protected Left	92.7										
850	72250	Area type is residential	85.0										
812	65853	Left turn percentages	81.2										
811	65772	Intersection spacing	81.1										
683	46581	Right turn percentages	68.3										
645	41538	Merge on exit side	64.5										
605	36542	Bicycle facilities	60.5										
561	31472	Arterial Posted Speed	56.1										
477	22753	Operations	47.7										
467	21762	Emissions	46.7										
429	18404	Safety	42.9										

C. Emissions:

As with the other variables, Table 20 ranks the variables according to the μ values and respective β . Intersection spacing was the variable that was found to increase emissions the most. This is expected, since longer segment lengths results in more driving and thus higher emissions. On the other hand, some variables that were associated with better performance in terms of operations also resulted in lower emissions. Those variables are Size and Shared Turns.

Table 20. Ranking of μ for the All Variables and Associated β – Emissions

Variable	μ	β
Intersection spacing	840.500	1.000
Volume increments (multipliers)	202.910	1.000
Protected Left	5.450	0.277
Operations	4.315	0.815
Left turn pockets	3.440	0.966
Bicycle facilities	1.030	0.880
Mast-arm signal display	0.390	0.379
Parking within 330 feet from stop bar	-0.020	1.000
Bus bay within 330 feet from stop bar	-0.070	0.778
Merge on exit side	-0.090	0.818
Median island	-0.640	0.941
Emissions	-1.027	0.189
K factor	-2.000	0.820
Safety	-3.097	0.682
Area type is residential	-7.110	0.929
Arterial Posted Speed	-24.650	1.000
Right turn percentages	-81.460	0.860
Left turn percentages	-136.920	0.846
Size	-707.160	0.749
Shared left turn	-766.790	1.000
Shared right turn	-856.920	1.000

Higher turning percentages were also related to lower emissions, as can also be seen on Figure 15. This happened because, in this case study, the through movements were more often the critical ones, so that higher percentages of left turns would improve overall performance.

Figure 15 also shows the relevance and variability of the Size variable, which was also observed for the other performance measures.

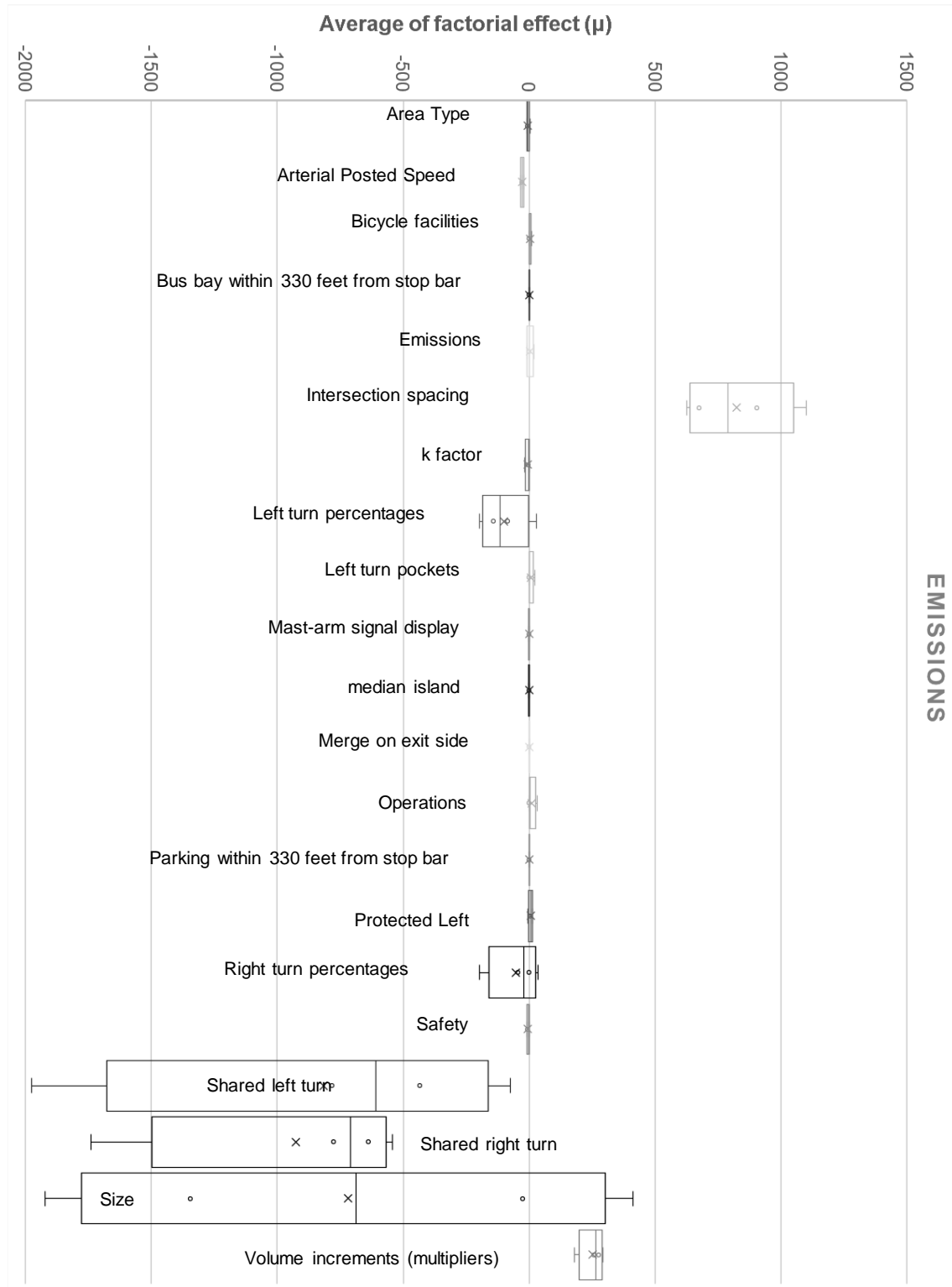


Figure 15: Variability of μ for each variable – Emissions

Table 21 and Table 22 show the analysis for μ^* . When accounting for positive and negative factorial effects on emissions, Size becomes the most important factor in the analysis, despite its large standard deviation. Traffic Volumes were found to play a significant role in the model, as they did with the other performance measures. Safety-only was not found to affect emissions.

Table 21. Ranking and Confidence Interval of μ^* for All Variables – Emissions

Variable	Lower Bound	μ^*	Upper Bound	Std. Dev σ
Size	315.489	944.760	1574.031	1015.289
Shared right turn	570.082	856.920	1143.758	462.795
Intersection spacing	674.172	840.500	1006.828	268.360
Shared left turn	351.888	766.790	1181.692	669.419
Volume increments (multipliers)	140.262	202.910	265.558	101.079
Left turn percentages	77.298	161.760	246.222	136.273
Right turn percentages	17.930	94.700	171.470	123.864
Arterial Posted Speed	21.019	24.650	28.281	5.858
Protected Left	2.684	19.670	36.656	27.406
Area type is residential	1.814	7.650	13.486	9.417
Emissions	-0.570	5.443	11.455	9.701
Operations	-0.882	5.297	11.475	9.969
Safety	0.706	4.544	8.382	6.192
Left turn pockets	-1.151	3.560	8.271	7.600
K factor	-1.079	2.440	5.959	5.678
Bicycle facilities	-1.003	1.170	3.343	3.507
Mast-arm signal display	-0.417	1.030	2.477	2.334
Median island	-0.453	0.680	1.813	1.828
Merge on exit side	-0.031	0.110	0.251	0.228
Bus bay within 330 feet from stop bar	-0.031	0.090	0.211	0.195
Parking within 330 feet from stop bar	-0.006	0.020	0.046	0.042

Among the three performance measures, the emissions was the one that was clearly affected by each variable, with statistical confidence, as shown in Table 22. It can be noticed that the H value

is higher, while Tukey Lines are generally shorter, which means that variables are more differentiated among themselves, at 95% confidence.

Table 22. Kruskal Wallis Test – Emissions

Multiple comparisons (Pairwise)				KRUSKAL-WALLIS TABLE	
				Chi	16.92
				H	550.92
T	T ² /n	Variable	R̄	Tukey Lines	
1831	335256	Intersection spacing	192.6		
1908	364046	Shared right turn	190.8		
1926	370948	Size	183.1		
1822	331968	Shared left turn	182.2		
1619	262116	Volume increments (multipliers)	161.9		
1599	255680	Left turn percentages	159.9		
1393	194045	Right turn percentages	139.3		
1347	181441	Arterial Posted Speed	134.7		
1240	153760	Protected Left	124.0		
1079	116424	Area type is residential	107.9		
825	68063	Emissions	82.5		
767	58829	Safety	80.9		
809	65367	Operations	76.7		
708	50126	Left turn pockets	70.8		
631	39816	k factor	63.1		
455	20703	Mast-arm signal display	61.2		
612	37393	Median island	46.8		
468	21856	Bicycle facilities	45.5		
413	17057	Merge on exit side	41.3		
390	15210	Bus bay 330 feet from stop bar	39.0		
315	9891	Parking 330 feet from stop bar	31.5		

CHAPTER 5: CONCLUSIONS AND RECOMMENDATIONS

The goal of this study was to develop a signal timing optimization algorithm that can consider mobility, safety, and environmental measures simultaneously on coordinated arterials. To attain this goal, an emissions model was developed (Part A of this report) and a set of crash prediction equations were identified for use in the optimization. The selected safety model has the advantage of considering geometry and control aspects, while its structure, analogous to the HSM's, allows for local calibration of existing parameters, as well as inclusion of new factors (CMFs), that can be derived from before-after studies using field data or microsimulation.

This research created and coded a tool in the HCS engine (which includes the TRANSYT-7F optimization tool), capable of optimizing signal timing and coordination on arterials. The resulting software is available to users as part of the HCS – Streets module.

A sensitivity analysis was undertaken to gain a better understanding of the interactions among variables and the tradeoffs between safety, mobility, and emissions. This analysis was conducted using the Factorial Effects method, by testing key variables that affect safety, mobility, emissions outputs separately. It was concluded that, while some variables are noticeably more significant than others, the effect of several of them is highly dependent on other variables, so that the individual degree of importance of each variable to the model cannot be fully ranked, at 95% confidence.

Nevertheless, the Size of the intersection, as defined by the number of lanes on the arterial, was found to largely affect all three performance measures. In the case of safety, large intersections with short left turn pockets were associated with a much higher number of angle

and rear-end crashes, especially when hourly and/or annual volumes are higher. This effect can be mitigated with the used of shared left-turns.

For the studied case, permitted left turns improved operations without compromising safety. Higher speeds were associated with slightly more crashes, although they did not significantly affect overall performance. Intersection spacing mostly affected emission levels, as the higher the segment lengths, the more gases are emitted. The effect of shared turns was highly dependent on the volume and turning percentage levels. For most scenarios in the case study, the through movements were the critical ones, so that shared turns enhanced overall performance, improving mobility, safety and emissions.

Demand level variables, such as the volume multipliers, are directly correlated to delay and emissions. The k factor affects the AADT values, which are used by the safety model only, and have a high level of influence. The weight schemes had little influence on the optimal results, regardless of the importance given to a particular performance measure.

A limitation of this study is that many safety-only related variables could not be fully tested for their effect on other performance measures. The presence of bus bays, parking or bicycles facilities, for example, were analyzed in terms of safety impacts only, due to the large variability and uncertainties of operation effects of these variables. Likewise, merges at the outbound legs of the intersection were considered simply as a slight reduction on lane width. Full lane drops weren't used, to avoid the occurrence of oversaturated conditions and spillbacks, which were beyond the scope of this research.

REFERENCES

1. State of New Jersey Department of Transportation, <http://www.state.nj.us/transportation/refdata/accident/policecrashtypedef.shtm>. Accessed Mar. 22, 2015.
2. Minimum uniform crash criteria, http://www.mmucc.us/mmucc-training/lessons/crashdamage/manner_files/manner05.htm. Accessed Mar. 22, 2015.
3. City of Fort Collins, http://www.fcgov.com/traffic/approach_crashes.php. Accessed Mar. 22, 2015.
4. Poch, M., and F. Mannering. Negative Binomial Analysis of Intersection-Accident Frequencies. *Journal of Transportation Engineering*, Vol. 122, 1996, pp. 05-113.
5. Mitra, S., Chin, H. C., and M. Quddus. Study of Intersection Accidents by Maneuver Type. In *Transportation Research Record 1784*, TRB, National Research Council, Washington, D.C., 2007, p. 43-50.
6. Lambert, D. Zero-Inflated Poisson Regression with an Application to Defects Manufacturing. *Technometrics*, Vol. 34, No. 1, 1992, pp. 1-14.
7. Chin, H., and M. Quddus. Applying the random effect negative binomial model to examine traffic accident occurrence at signalized intersections. *Accident Analysis and Prevention*, Vol. 35, 2003, pp. 253–259.
8. Wang, X. S., and M. Abdel-Aty. Temporal and spatial analyses of rear-end crashes at signalized intersections. *Accident Analysis and Prevention*, Vol. 38, 2006, pp. 1137-1150.
9. Agbelie, B., and A. Roshandeh. Impacts of Signal-Related Characteristics on Crash Frequency at Urban Signalized Intersections. *Journal of Transportation Safety & Security*, Vol. 7, 2015, pp. 199-207.
10. Archer, J., and I. Kosonen. The potential of micro-simulation modeling in relation to traffic safety assessment. *Proceeding, ESS Conference*, Hamburg, Germany, 2000.
11. Drummond, K., L. A. Hoel, and J. S. Miller. *A Simulation-based Approach to Evaluate Impacts of Increased Traffic Signal Density*. Research report of Virginia, Transportation Research Council, Charlottesville, Virginia, 2002.
12. Archer, J. *Methods for the Assessment and Prediction of Traffic Safety at Urban Intersections and their Application in Micro-simulation Modeling*. PhD dissertation, Division of Transport and Logistics, Royal Institute of Technology, Stockholm, Sweden, 2004.

13. Ozbay, K., H. Yang, B. Bartın, and S. Mudigonda. Derivation and validation of new simulation-based surrogate safety measure. In *Transportation Research Record 2083*, TRB, National Research Council, Washington, D.C., 2008, pp. 105–113.
14. Archer, J., and W. Young. Traffic micro-simulation approach to estimate safety at unsignalized intersections. *Presented at 89th Transportation Research Board Annual Meeting (CD ROM)*, Washington, D.C., 2010.
15. Gettman, D., L. Pu, T. Sayed, and S. Shelby. *Surrogate Safety Assessment Model and Validation*. Final report. FHWA-HRT-08-051. FHWA, U.S. Department of Transportation, 2008.
16. Saleem, T., B. Persaud, A. Shalaby, and A. Arize. Can Microsimulation Be Used to Estimate Intersection Safety? In *Transportation Research Record 2432*, TRB, National Research Council, Washington, D.C., 2014, pp. 142–148.
17. Essa, M., and T. Sayed. Simulated Traffic Conflicts. Do They Accurately Represent Field-Measured Conflicts? In *Transportation Research Record 2514*, TRB, National Research Council, Washington, D.C., 2015, pp. 48-57.
18. Shahdah, U., Saccomanno, F., and B. Persaud. Application of traffic microsimulation for evaluating safety performance of urban signalized intersections. *Transportation Research Part C*, Vol. 60, 2015, pp. 96-104.
19. Pirdavani, A., T. Brijs, T. Bellemans, and G. Wets. A simulation-based traffic safety evaluation of signalized intersections. *Proceedings of the Road Safety on Four Continents Conference*, 2010, pp. 1229–1239.
20. Stevanovic, A., J. Stevanovic, J. So, and M. Ostojic. Multi-criteria optimization of traffic signals: Mobility, safety and environment. *Transportation Research Part C*, Vol. 55, 2015, pp. 46-68.
21. So, J., S. Hoffmann, J. Lee, F. Busch, and K. Choi. A Prediction Accuracy-Practicality Tradeoff Analysis of the State-of-art Safety Performance Assessment Methods. *Transportation Research Procedia*, Vol. 15, ISEHP 2015, pp. 794-805.
22. Florida Department of Transportation, <http://www.dot.state.fl.us/rddesign/QA/Tools.shtm>. Accessed by March 21st, 2015.
23. American Association of State Highway and Transportation Officials, *Highway Safety Manual*, 2010.
24. Turner, S., R. Singh, and G. Nates. *Crash prediction models for signalized intersections: signal phasing and geometry*. NZ Transport Agency research report 483, 2012.
25. Beasley, D., D. Bull, and R. Martin. An Overview of Genetic Algorithms: Part 1, Fundamentals”. *University Computing*, Vol. 15, No. 2, 1993, pp. 58-69.

26. Coley, D. *An Introduction to Genetic Algorithms for Scientists and Engineers*. World Scientific, 1999.
27. Azar, S., B. Reynolds, and S. Narayanan. Comparison of Two objective Optimization Techniques with and within Genetic Algorithm. *Proceedings, ASME Design Engineering Technical Conferences*, 1999.
28. Yang, W., L. Zhang, L. Zhang, and H. Shi. *A Golden Ratio-Based Genetic Algorithm and Its Application in Traffic Signal Timing Optimization for Urban Signalized Intersections*, 2013.
29. Kuehl, R. *Design of Experiments: Statistical Principles of Research Design and Analysis 2nd*. Duxbury Press, 1999.
30. Trucano, T. G., L. P. Swiler, T. Igusa, W. L. Oberkampf, and M. Pilch. Calibration, validation and sensitivity analysis: What's what. *Reliability Engineering & System Safety*, Vol. 91, 2006, pp. 1331-1357.
31. Saltelli, A., S. Tarantola, F. Campolongo, and M. Ratto. *Sensitivity analysis in practice: A guide to assessing scientific models*. John Wiley & Sons Ltd, The Atrium, Southern Gate, Chichester, UK, 2004.
32. Santner, T. J., B. J. Williams, and W. I. Notz. *The Design and Analysis of Computer Experiments*, Springer-Verlag, New York, NY, 2003.
33. Saltelli, A., K. Chan, and M. Scott. *Sensitivity Analysis*. Wiley, New York, NY, 2000.
34. Morris, M. D. Factorial Sampling Plans for Preliminary Computational Experiments. *Technometrics*, Vol. 33, No. 2, 1991, pp. 161-174.
35. Campolongo, F., J. Cariboni, and A. Saltelli. An effective screening design for sensitivity analysis of large models. *Environmental Modelling & Software*, Vol. 22, No. 10, 2007, pp. 1509-1518.
36. Nunes, D. F. *Procedimento para Análise de Sensibilidade do Programa HDM-4*. Master thesis, São Carlos School of Engineering, University of São Paulo, Brazil, 2012.
37. Montgomery, D. C., and G. C. Runger. *Applied Statistics and Probability for Engineers*. Wiley, USA, 2014.